

Technical Report No. TR-55

April 1984

Analysis of Productivity and Cost of Forestry Transportation

**PART TWO: Theoretical Analysis of the Impact
of Vehicle Operating Conditions on Power Losses,
and Experimental Determination of the Resistance
Forces Attributable to Oil Churning**

D.A. Ljubic

Analysis of Productivity and Cost of Forestry Transportation

**PART TWO: Theoretical Analysis of the Impact
of Vehicle Operating Conditions on Power Losses,
and Experimental Determination of the Resistance
Forces Attributable to Oil Churning**

D.A. Ljubic

Technical Report No. TR-55
April 1984

Ce rapport technique est disponible en français

FERIC **FOREST ENGINEERING RESEARCH INSTITUTE OF CANADA**
INSTITUT CANADIEN DE RECHERCHES EN GÉNIE FORESTIER

ACKNOWLEDGMENTS

The analysis written up in this second part of our research series is the outcome of cooperative efforts on the part of two forestry enterprises, different manufacturers of power transmission lubricants and the Forest Engineering Research Institute of Canada (FERIC).

The author is sincerely grateful to the management, drivers and mechanics of Industries James Maclaren Inc. and of CIP Inc., with particular thanks for assistance and support in the research effort going to B. Hunt, E. Hébert, J.C. Léonard, G. Brunet, E. Scott and G. Ouellet of Maclaren and to K. Allen, W. Brown, C. Fournier, A. Vallée, G. Valiquette and J.P. Carpentier of CIP.

Among the other contributors were the experts at Eaton Corporation, Pacific Truck and Trailers, Mack Canada Inc., Canadian Kenworth Company, Société Canadienne des Pneus Michelin Ltée, Sentinel Lubricants Corporation, Charles Tennant and Co. Ltd. (Ultron oil), Emery Industries (Emgard oil) and Lubrizol Corporation (Uniroyal oil). H. Ruhl Machinery Ltd., particularly in the persons of Muhammad G. Rana and Ted Jurca, took part in developing instruments, thereby lending invaluable assistance for the design of special instrumentation for use on moving vehicles.

Particular contribution in the field of instrument and computer work has been made by the FERIC's researcher P. Giguère to whom the author is appreciative and thankful.

Lastly, as this was a FERIC team effort, the author wish to thank Jean Courteau whose hard, precise work and systematic approach were so instrumental in the success of the investigations. Thanks are also in order for D. MacGregor, M. St-Amour and K. Hadley.

TABLE OF CONTENTS

	Page
ACKNOWLEDGMENTS	i
LIST OF FIGURES	iv
LIST OF TABLES	vi
SUMMARY	vii
A. INTRODUCTION	1
B. THE NEED FOR A SYSTEMATIC FORESTRY TRANSPORTATION RESEARCH PROGRAM	1
C. TRANSPORT CYCLE ANALYSIS	2
D. THE THEORETICAL AND EXPERIMENTAL ANALYSIS OF THE BASIC PARAMETERS OF A MOVING VEHICLE	4
D.1. THEORETICAL ANALYSIS OF THE BASIC PARAMETERS OF A ROAD VEHICLE	5
D.1.0. Vehicle mass G_T (kg)	6
D.1.1. Specific power N_{ESP} (kW/t)	7
D.1.2. Power transmission efficiency coefficient η_{PL}	7
D.1.3. Engine performance ratings at full and partial load	12
D.1.4. Power transmission ratings	13
D.1.5. Wheel radii	13
D.1.6. Center of gravity coordinates	13
D.1.7. Moments of inertia	14
D.1.8. Air resistance coefficient C_{FRO}	14
D.1.9. Rolling resistance coefficient f_{RR}	16
D.2. TRACTIVE EFFORT F_T (daN)	18
D.2.1. Forces of resistance related to the drive train and wheel bearings friction	23
D.2.2. Force of rolling resistance F_{RR}	24
D.2.3. Force of air resistance F_{AR}	24
D.2.4. Inertia forces F_I	24
D.3. EQUATION OF A MOVING VEHICLE (DUTY CYCLE EQUATION)	25
E. SAMPLE ENERGY BALANCE FOR A ROAD VEHICLE	29
F. COMMENTS ON COMPONENT LUBRICATION THEORY AND THE EXPERIMENTAL RESULTS FROM AN INVESTIGATION OF DRIVE TRAIN POWER LOSSES	31

	Page
F.0. COMMENTS ON COMPONENT LUBRICATION THEORY	31
F.1. EXPERIMENTAL RESULTS REGARDING DRIVE TRAIN POWER LOSSES	32
F.1.0. Verification of the methodology and accuracy of resistance determinations and consumption measurements	32
F.1.1. Operating factors affecting resistance forces	32
G. INTERPRETATION OF RESULTS	46
G.0. DETERMINING COEFFICIENT η_{OCL} FOR OIL CHURNING LOSSES IN A POWER TRANSMISSION SYSTEM	46
G.1. SAMPLE APPLICATIONS UNDER ACTUAL OPERATING CONDITIONS	47
G.2. COMPARISON OF RESULTS FOR STANDARD OIL AND SYNTHETIC OIL UNDER ACTUAL OPERATING CONDITIONS	48
G.3. STARTING AND OPERATING WITH COLD OILS	49
H. SAMPLE CALCULATION OF POTENTIAL FUEL SAVINGS IN TERMS OF OPERATING CONDITIONS	54
H.0. CALCULATING POTENTIAL FUEL SAVINGS DURING WINTER MONTHS (-20°C MEAN AMBIENT TEMPERATURE)	54
H.1. CALCULATING POTENTIAL FUEL SAVING DURING SUMMER MONTHS (+15°C MEAN AMBIENT TEMPERATURE)	55
I. CONCLUSION	57
J. APPENDIX	58
J.0. DETERMINING THE MOMENT OF INERTIA J_{WT} OF A TIRE WITH WHEEL (daN·m·sec ²)	58
J.1. TESTING METHODS	60
J.2. INSTRUMENTATION	61
DEFINITIONS OF SYMBOLS	72
REFERENCES	79

LIST OF FIGURES

	Page
Figure 1. Transport cycle.	2
Figure 2. Duty cycle research plan.	3
Figure 3. Example of distribution of the mass of a transport vehicle on a stationary scale.	6
Figure 4. Example of determining the distribution of the mass of a transport vehicle using portable scales.	7
Figure 5. Effect of ambient temperature on air density coefficient $\rho(\rho/\rho_0)$.	15
Figure 6. Effect of road curve radii on fuel consumption.	17
Figure 7. Ground balance of traction wheel.	19
Figure 8. Example of standard utilization of engine torque.	20
Figure 9. Tractive forces road equilibrium diagram.	25
Figure 10. Energy balance on a straight paved road (G.C.W. 60 000 kg steady speed of 56 km/h, direct drive, summer conditions dry & +32°C).	29
Figure 11. Truck energy balance on a gravel road (summer).	30
Figure 12. Truck energy balance on a snow-covered icy gravel road.	30
Figure 13. Diagram of oil churning resistance to engine and drive train rotation (drive wheels lifted off the ground).	34
Figure 14. Diagram of fuel consumption for standard oil.	36
Figure 15. Diagram of fuel consumption in terms of oil temperatures (transmission and two axles combined). Comparison of the three test oils.	38
Figure 16. Establishment of drive train efficiency coefficients.	39
Figure 17. Establishment of drive train efficiency coefficients in terms of oil temperatures for synthetic oils 'A' and 'B'.	40
Figure 18. Kinematic viscosity ASTM D-445 centistokes in terms of temperature (°C).	42

	Page
Figure 19. Relationship between viscosity, oil temperature and fuel consumptions (from oil churning only) for standard oil.	50
Figure 20. Relationship between viscosity oil temperature and fuel consumptions (from oil churning only) for synthetic oil 'B'.	51
Figure 21. Relationship between viscosity, oil temperature and fuel consumptions (from oil churning only) for synthetic oil 'A'.	52
Figure 22. Build-up of transmission and rear axle oil temperatures during winter operation.	53
Figure 23. Build-up of transmission and rear axle oil temperatures during summer operation.	53
Figure 24. Diagram of a wheel rolling on a decline.	58
Figure 25. Cross section of pulse sending unit used for speed measurements.	65
Figure 26. Diagram of batch volumetric fuelmeter (FERIC).	65
Figure 27. Diagram of batch weight fuelmeter (FERIC).	66
Figure 28. Diagram of continuous volumetric fuelmeter (RUHL).	67
Figure 29. FERIC initial instrument group.	68
Figure 30. FERIC DATAMASTER. Front view: The displays are either LED or LCD. A 6-channel thermocouple selector is located to the right of the on/off switch.	69
Figure 31. FERIC DATAMASTER. Rear view: Outlets for the pulse sending unit, power supply and Datalogger wires. The thermocouple outlets are located beneath the three VDC terminals.	69
Figure 32. Connection scheme and diagram of measuring and logging instruments mounted on the vehicle.	70
Figure 33. Diagram of equipment used to heat drive train components.	71

LIST OF TABLES

	Page
Table 1. Comparison of power losses in the transmission and drive axles of a logging truck as calculated from fuel consumption measurements and by the coast down method (for three different lubricating oils).	33
Table 2. Comparison of fuel consumptions (kg/h) through oil churning losses for different oils in the transmissions and rear axles.	44
Table 3. Comparison of fuel consumptions on the road (loaded vehicle) for standard oil and for pure synthetic oil 'A' in the transmission and drive axles (all other conditions being comparable).	44
Table 4. Comparison of fuel consumptions (kg/h) through oil churning losses in the transmissions and rear axles for a standard and synthetic oils.	45
Table 5. Comparison of fuel consumptions (kg/h) through oil churning losses in the transmissions and rear axles.	45

SUMMARY

Industry personnel in the road construction and transportation sectors are fully aware that road design and surface, the selection and handling of trucks and truck components and driver performance are all factors affecting wood transportation costs. They are often frustrated by the lack of substantive information required to make decisions and convince both financial and purchasing officers that considerable benefit could be reaped from a little additional investment in roads, equipment and driver training. FERIC has undertaken a series of studies designed to gather such information. Its research program offers the promise of providing data that can be put to immediate use to reduce the fuel and maintenance costs of present road transportation operations and to guide its members in the selection of optimal truck-road combinations for the future.

The first part of this report deals with the theory of energy balance of a moving vehicle. This theory will provide the basis for future investigations taking the form of duty cycle analyses. The second part of the report examines the results of a study of power losses through oil churning in the power transmission system.

The following is a summary of our research findings:

- both the methodology used and the accuracy of the results are borne out by two entirely different methods of investigation (see Table 1).
- preliminary findings that indicated fuel savings of 3 to 7% through the proper choice or heating of the power transmission lubricant (see technical report TR-53) are confirmed by the results of a systematic investigation written up in this report. An annual average fuel savings of 8% was established -- solely on the basis of oil churning resistances -- by artificially maintaining the oil temperature at 80°C. This gain will undoubtedly be even greater if the effect of mechanical (internal) friction with applied engine torque is taken into account.
- with torque applied and under the same operating conditions, a fuel saving of 0.8% was found with the use of synthetic oil "A" as opposed to standard oil. This suggests that at high temperatures synthetic oils have some positive effect on mechanical friction in the power transmission system.
- given an ambient temperature of -20°C, it takes some three hours in service to achieve stabilized oil temperatures, proving that the forestry industry seldom operate trucks under the most efficient working conditions, particularly during winter months. This indicates the need for preheating transmission oils, just as is done for the engine oil.
- there may be a practical means of preheating the power transmission oils using engine coolant or exhaust gases. FERIC will investigate these possibilities.

Other reports in this series will follow.

A. INTRODUCTION

This second report in the series titled Analysis of Productivity and Cost of Forestry Transportation develops the theory of the relationships for the study of the energy balance of a transport vehicle at any point in its duty cycle and indicates the areas to be investigated in the next phases of the FERIC transport research program. It goes on to give the results of the first experimental phase which deals with the power losses through oil churning in the transmission and rear axles.

The basic aims of the test program were first to investigate and determine the actual conditions under which forest vehicles operate and then to examine how these conditions affect the efficiency of the system that transmits power between the engine and the traction wheels. This efficiency is a function of two types of losses: oil churning losses (independent of the torque transmitted) and direct loss through transmitted torque, caused by mechanical friction throughout the system. The oil churning losses are examined in the second part of this report.

Given that viscosity is the primary determinant of churning resistance, two methods were used to modify the viscosity factor so as to examine its effect on the power loss coefficients. We began by analyzing several oils featuring different viscosity properties and went on to make controlled changes to their viscosities by devising an oil preheating and heating system (see appendix). This allowed us to analyze the law of changing resistances (fuel consumptions) as a function of temperatures and to derive power loss coefficients.

This study should not be construed as an evaluation of different brands or types of oils. Our tests focused on the performances achieved under controlled, instantaneous conditions and does not constitute an analysis of the durability of the oils or of the power transmission components with their use.

B. THE NEED FOR A SYSTEMATIC FORESTRY TRANSPORTATION RESEARCH PROGRAM

The Canadian forestry industry is confronted with very particular operating conditions:

- the climate is harsh and variable;
- mills and felling sites are often far apart and the distances are increasing each year;
- private road networks were not designed for optimal transportation efficiency and cost;
- the necessary specification alternatives are not always available from the manufacturers, who produce for North America's mass market;
- vehicle overloading is very common;
- in many cases the lack of information and understanding of the magnitude of the relationships between system variables prevents management, drivers and mechanics from optimizing the transport cycle.

Given that operation, maintenance and repair account for up to half of the cost of wood shipped to Canadian mills, it is essential that the forestry industry undertake an in-depth study of the transport cycle. This presupposes the development of research methods for measuring the basic coefficients and the relationships between variables. Once these coefficients have been individually determined, they can be combined to optimize an existing transport cycle or else to provide for a more scientific analysis as a base to optimize future operations.

This is precisely the aim of the long-term forestry transportation research program to which FERIC is committed.

C. TRANSPORT CYCLE ANALYSIS

A regular transport cycle is a combination or arrangement of a number of key factors that affect productivity and costs. Figure 1 identifies the most important of these factors which are:

- transport unit and its components
- road design and surface
- atmospheric conditions
- driving technique
- quality of maintenance
- operational set-up

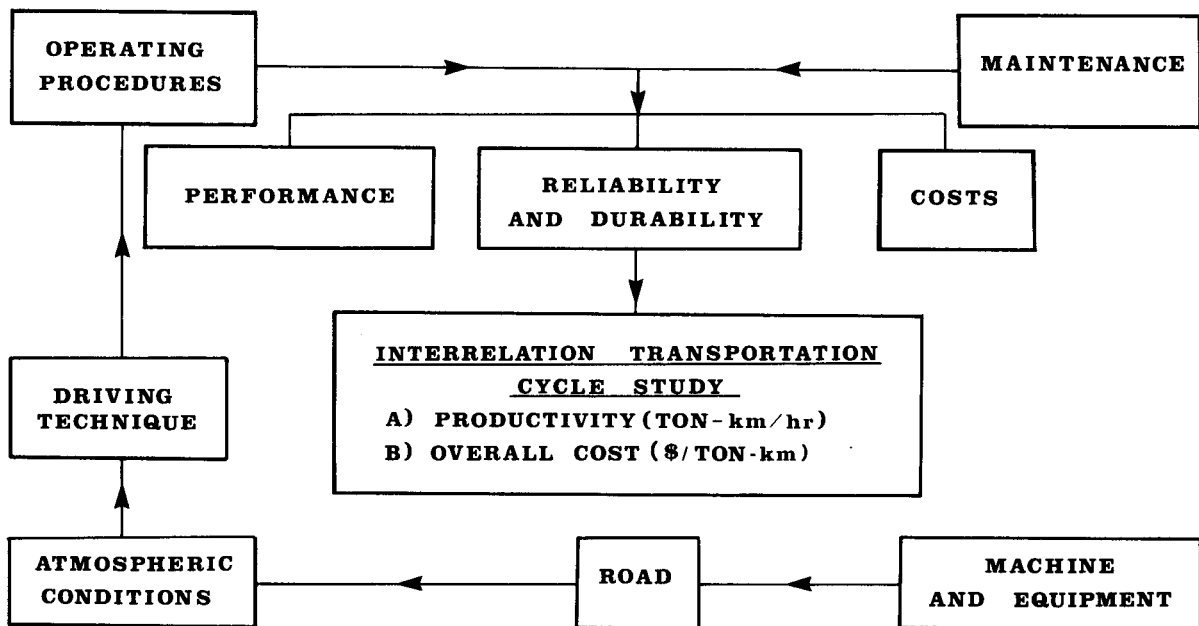


Figure 1 : Transport cycle.

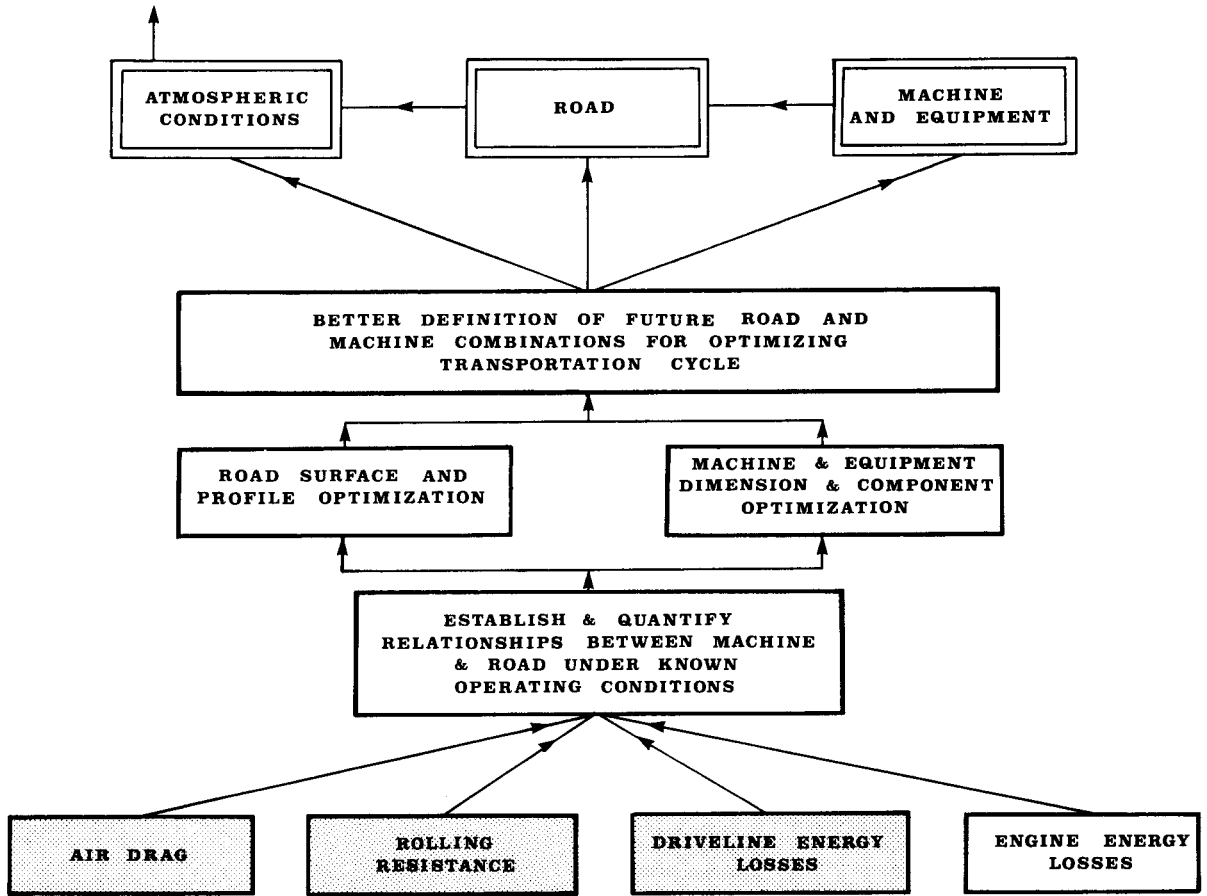


Figure 2: Duty cycle research plan.

The interplay of these and other factors determines the performance, reliability and durability of a transport unit and thus the total cost of hauling wood from the forest.

Figure 2 charts areas FERIC has studied to date (shaded blocks) and those slated for study in the future. This report (Part II) presents some partial findings with regard to power losses and coefficients of friction in the drive train (transmission and rear axles) through oil churning.

Part III will give preliminary results concerning power losses and rolling and air resistance coefficients. Engine power losses and coefficients of mechanical resistance will be considered later on in the research program.

In 1984 FERIC will purchase and install instruments to measure various factors relative to a moving truck, thereby gaining the means to conduct a comprehensive study of the duty cycle of a truck-trailer combination. Once recorded and interpreted, these data will be used to investigate the operator-machine-environment relationship, which in turn will make it possible to determine the optimum combinations of these factors for present or future operations.

D. THE THEORETICAL AND EXPERIMENTAL ANALYSIS OF THE BASIC PARAMETERS OF A MOVING VEHICLE

While the physical laws and relationships relating to the performance and energy balance of a moving vehicle are well known, many of the equations contain important coefficients which are dependent upon the conditions under which the vehicle is being operated. A prime purpose of the FERIC transportation research program is to determine these coefficients for the transport unit options, the weather and the road conditions which exist in the logging industry of central and eastern Canada. Hence FERIC's decision to use regular logging trucks in their working environment as the test equipment and test laboratory.

This decision brought with it some measurement problems. It has not always been possible to measure some factors by the most direct route so the interrelationships between variables have been studied to find the relevant factors which can be measured and which then permit the determination of the desired unknown by calculation.

This section of the report defines the basic equations relating to the performance and energy balance of a moving vehicle. In some cases, the substitution of interrelationship was necessary and the logic exercises of these has been shown. Finally, the factors which have already been measured during this research study have been identified and some explanation has been given about the plans to measure those to be determined in the future stages. Thus, the theory and research steps of the complete study, of which this report covers only the second stage, are outlined.

At first glance, there are a great number of symbols used in the formulae which follows. It may help the reader to know that the basic ISO symbols are used throughout. Thus, for example, N always relates to power and η is always an efficiency coefficient. As there can be several physical components influencing the basic factors, a lettered symbol subscript code has been added. As much as possible, this is composed of the first letters in the key words defining the area or conditions to which the symbol relates. Thus, for example, in η_a , the a refers to the coefficient of power loss caused by engine acceleration, and in η_{EAT} , the EAT refers to the coefficient of power loss owing to an increment of engine ambient temperature.

D.1. THEORETICAL ANALYSIS OF THE BASIC PARAMETERS OF A ROAD VEHICLE

The main characteristics that determine the performance and energy balance of a moving vehicle are enumerated below:

- D.1.0. Vehicle mass G_T in kg.
- D.1.1. Specific power N_{ESP} , i.e. the number of kilowatts per ton hauled, kW/t*.
- D.1.2. Power transmission efficiency coefficient η_{PL} .
- D.1.3. Engine performance ratings at full and partial load.
- D.1.4. Power transmission ratings.
- D.1.5. Wheel radii:
 - D.1.5.1. No-load radius r_{FR} , m (meters).
 - D.1.5.2. Live radius (static) r_{LS} .
 - D.1.5.3. Live radius (kinematic) without applied torque r_{LK}^0 .
 - D.1.5.4. Live radius (dynamic) with applied torque r_{LD}^M .
- D.1.6. Center of gravity coordinates.
- D.1.7. Moments of inertia:
 - D.1.7.1. Moment of inertia of wheel with tire J_{WT} in $daN \cdot m \cdot sec^{2**}$.
 - D.1.7.2. Moment of inertia of all wheels with tires $J_{\Sigma WT}$ in $daN \cdot m \cdot sec^2$.
 - D.1.7.3. Drive train moment of inertia J_{DT} in $daN \cdot m \cdot sec^2$.
 - D.1.7.4. Moment of inertia of wheels plus drive train J_{WTDT} in $daN \cdot m \cdot sec^2$.
 - D.1.7.5. Engine moment of inertia J_E in $daN \cdot m \cdot sec^2$.
- D.1.8. Air resistance coefficient C_{PRO} .
- D.1.9. Rolling resistance coefficient f_{RR} .

Let us take a closer look at some of these factors.

* From this point on, all sizes and units will be expressed in the ISO system, meaning that some of the symbols used in technical report TR-53 will be changed.

** See appendix for method of determination.

D.1.0. Vehicle mass G_T (kg)

The total vehicle mass G_T (kg) is composed by the tare mass of the vehicle combination G_{TA} (kg) and the mass of the load G_L (kg).

Figure 3 shows a truck-trailer on a stationary scale with distribution of the mass. The mass per axle was established by advancing the vehicle on the scale.

Figure 4 shows a truck-trailer on a flat portion of road with the mass per axle weighed by two portable scales.

Numerous weighing operations by FERIC have shown weight values established on a stationary scale deviating on the order of $\pm 3\%$. Depending on the location of the weighing and several other factors, the deviation may be as high as $\pm 7\%$ for weights established on portable scales.

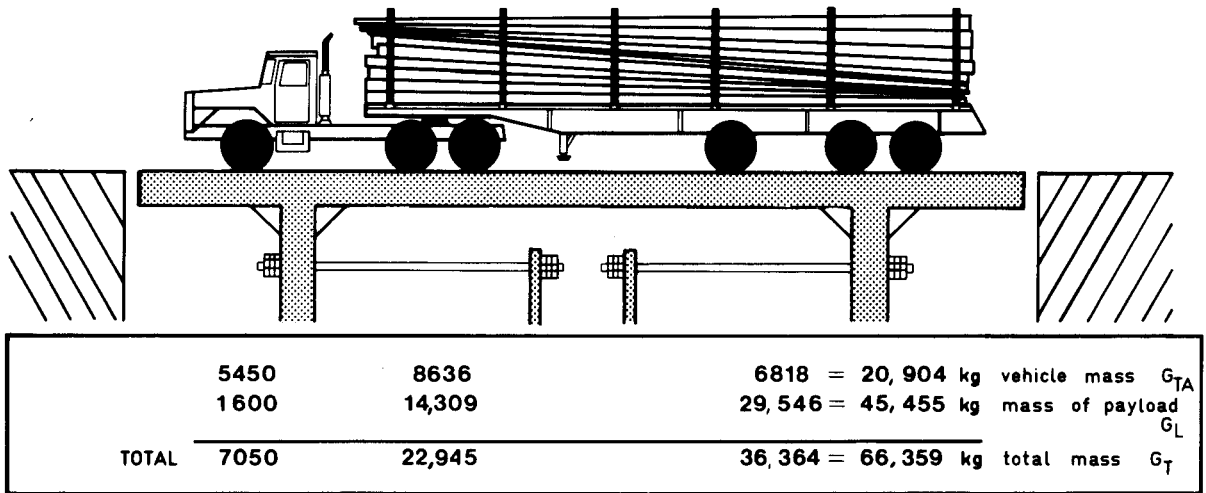


Figure 3: Example of distribution of the mass of a transport vehicle on a stationary scale.

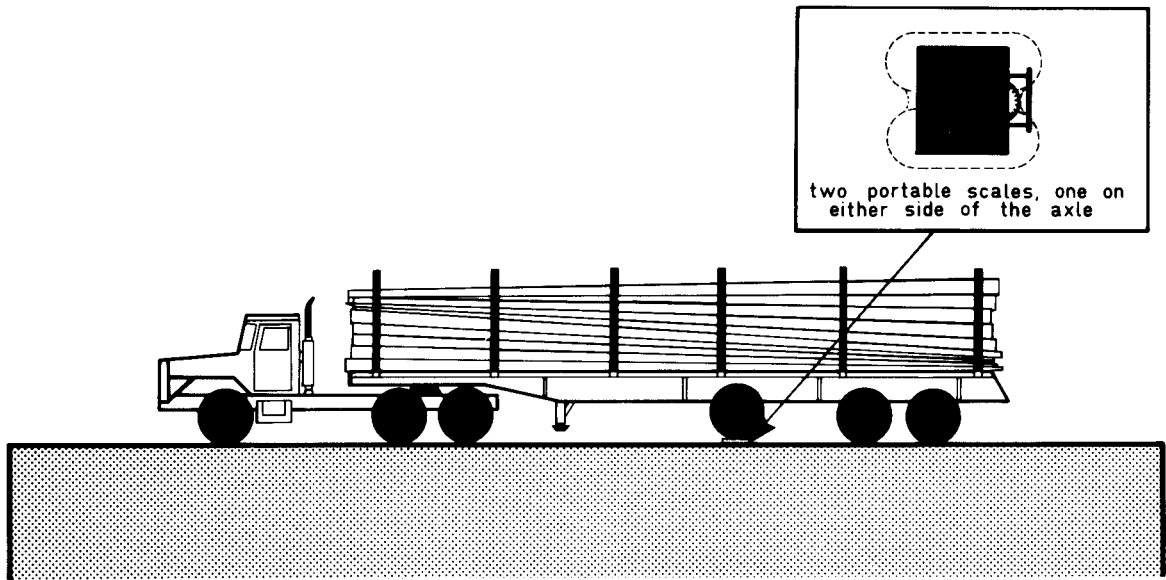


Figure 4: Example of determining the distribution of the mass of a transport vehicle using portable scales.

D.1.1. Specific power N_{ESP} (kW/t)

This designates the maximum effective power relative to total vehicle mass (N/kg or kW/t). Its value indicates whether or not a truck-trailer is overloaded, i.e. whether the power demand is excessive for the mass to be hauled and the operating conditions at hand. It is best illustrated by an example. With engine power of 298 kW (400 hp) and total mass of 91 tons, the specific power N_{ESP} is $298/91 = 3.27$. If this figure is any higher, through increasing the engine size to 4.50, for instance, it means the road speed will increase and productivity will be enhanced (providing that the time gained can be used to increase the number of runs per shift). On the other hand, vehicle purchase and maintenance costs will be higher as well.

D.1.2. Power transmission efficiency coefficient η_{PL}

The impact of coefficient η_{PL} on vehicle power consumption and road performance is represented by the power at the wheels relative to the effective engine power (see sample energy balances in Figures 9-11). The power loss does not occur at one place but is built up by power lost at each active component of the transport unit. Knowledge of the location and magnitude of these power loss components is a prerequisite to decisions or actions which will reduce the power lost in the operation of a machine.

Using engine effective power N_{EF} as the point of reference for a discussion on power losses:

$$\eta_{PL} = \frac{N_W}{N_{EF}} = \eta_{EA} \cdot \eta_{DT} \cdot \eta_{TW} \quad (1)$$

- where:
- N_W power at the wheels, kW
 - N_{EF} effective power of engine without accessories, kW
 - η_{EA} overall efficiency coefficient of engine with accessories (excluding engine heat and mechanical losses)
 - η_{DT} drive train efficiency coefficient [transmission(s) and rear axles(s)]
 - η_{TW} traction wheel efficiency coefficient

Engine external power efficiency η_{EA} comprises

$$\eta_{EA} = \eta_a \cdot \eta_{EAT} \cdot \eta_{SL} \cdot \eta_{EC} \quad (2)$$

- where:
- η_a engine acceleration efficiency
 - η_{EAT} engine ambient temperature efficiency coefficient
 - η_{SL} efficiency coefficient attributable to height above sea level
 - η_{EC} engine accessories efficiency coefficient and is given by the equation:

$$\eta_{EC} = \frac{N_{OUT}}{N_{EF}} \quad (3)$$

where:

N_{OUT} output power (kW) of the engine mounted in the truck. This power can be determined by means of an engine torque meter mounted behind the transmission (taking account of the power loss in the transmission). This meter is among the instruments that will be mounted in test trucks for road vehicle duty cycle runs, which, among other things, will yield an exact determination of the efficiency coefficient of power loss through the engine accessories η_{EC} . This may amount to 15% of the engine effective power, which points to another avenue for research aimed at reducing power consumption.

The value of coefficient η_a is obtained by measuring the output power of the engine first at constant speed and then accelerating from low speed to higher speeds. When passing by the speed used in the first case we instantaneously measure the power. It is expected to lie between $\eta_a = 0.93$ and 0.95 . Given that oil temperature and oil grade affect this loss, these factors will also have to be investigated and an attempt made to optimize them.

Coefficient η_{EAT} can be determined experimentally by means of a truck roller dynamometer. It can also be determined on the road after first establishing the losses through the accessories (engine only) and matching the torque or power found against the power specified by the builder at the same rotating velocity, n_E (RPM). This is done by mounting a torque meter behind the transmission. Losses from operating at non-optimum engine temperature may go as high as 18% of the engine effective power and will thus be a very interesting area for investigation later in this study program.

In the case of super-charged engines, the height above sea level is not a factor in central and eastern Canadian logging operations as the coefficient η_{SL} is very close to one up to an elevation 2,000 meters. Thus it does not warrant further consideration in this study.

The efficiency coefficient of drive train losses η_{DT} represents the ratio of engine output power to power at the wheels

$$\eta_{DT} = \frac{N_W}{N_{OUT}} = 1 - \frac{N_{DT}}{N_{OUT}} \quad (4)$$

- where: - N_{DT} power loss in the transmission system, in kW
- N_{OUT} engine power output
- N_W power at the wheels

Coefficient η_{DT} can also be given by the product of the coefficients of losses in the transmission, universal joints, forward-rear axle and rear-rear axle.

$$\eta_{DT} = \eta_{TL} \cdot \eta_{UJ} \cdot \eta_{A1} \cdot \eta_{A2} \quad (5)$$

The drive train losses account for a large portion of engine power output N_{OUT} , particularly at low power when oil churning losses are the greatest.

From here on in this report, drive train losses owing to oil churning are given in terms of engine output power and of transmission, forward-rear axle and rear-rear axle oil temperatures for standard oil and two synthetic oils. The results are all based on an engine rotating velocity of 1,800 RPM. Naturally, these coefficients change as a function of drive train velocity. The law of change is set out in report TR-53.

The second component of energy losses through the power transmission, i.e. losses through mechanical friction, is directly proportional to the torque transmitted. A study of this component is part of the 1984 research program. At high powers it may be greater than the losses through oil churning.

Equation (6) is used for aggregate analysis of the elements of power transmission losses:

$$\eta_{DT} = \eta_{FR} \left(1 - \frac{F_{OC}^*}{F_{OUT}} \right) \quad (6)$$

- where:
- η_{FR} efficiency coefficient for calculating loss through friction in power transmission system (with applied torque)
 - F_{OC} force corresponding to oil churning loss in power transmission system, daN
 - F_{OUT} effort at engine output or transmission intake, daN

The efficiency coefficient for losses through mechanical friction in the torque transmission system η_{FR} is usually given as a function of the quantity and design of gears in mesh and the number of universal joints, without regard for rotating velocity, transmitted torque or oil type or temperature. This is merely an approximation which, in actual fact, does not reflect the real situation. This element will require separate analysis in terms of all these factors in order to determine how the effect can be minimized, thereby reducing power consumption and the wear of the power transmission components.

By way of an example, the following is one empirical means of determining the coefficient of friction losses η_{FR} in the power transmission system. This method disregards power transmission velocity, applied torque, oil type and oil temperature. The equation used is:

$$\eta_{FR} = \eta_{CG}^m \cdot \eta_{BG}^n \cdot \eta_{UJ}^o \quad (7)$$

* In report TR-53 this force is designated as P_{tp}^o but has been changed to conform with ISO terminology.

- where:
- η_{CG}^m efficiency of cylindrical gears in mesh ($\eta_{CG}^m = 0.98$ to 0.985)
 - η_{BG}^n efficiency of bevel gears in mesh ($\eta_{BG}^n = 0.975$ to 0.98)
 - η_{UJ}^o efficiency of universal joints ($\eta_{UJ}^o = 0.99$)
 - m, n, o the number of meshed cylindrical gears, meshed bevel gears and universal joints, respectively

Continuing our example, we will empirically determine η_{FR} by calculation on one of our test trucks:

- for two pairs of meshed cylindrical gears (modern transmission), $m = 2$; for one pair of meshed bevel gears (drive pinion in rear axle), $n = 1$; for three universal joints, $o = 3$. Thus, according to formula (7):

$$\eta_{FR} = 0.983^2 \cdot 0.978 \cdot 0.99^3 = 0.92$$

This approximate value will be used later to calculate cases of average power losses through resistances in the power transmission system.

Coefficient η_{FR} will be studied separately at a later time to determine the actual losses in the power for different transmission systems of a range of forest vehicles.

The efficiency coefficient of losses at the wheels η_{TW} can be written as follows:

$$\eta_{TW} = \left(\frac{M_{WD}}{M_A} \right) \cdot \frac{r_{LK}^o}{r_{LD}} \quad (8)$$

- where:
- M_{WD} moment at drive wheels (at the ground), daN·m
 - M_A moment applied to drive wheels (prior to loss at the ground) daN·m

Studies by a number of researchers show equation $\eta_{TW} = f(M_{WD})$ as being non-linear, with maximum efficiency reaching 90% (0.9). The formula below can be used to derive the maximum efficiency of a tire.

$$\eta_{MT} = 1 - 2 G_W (f_{OS} + \Delta f_{vr}) \lambda / 9.8182 \quad (9)$$

- where: - G_W rated load per wheel, kg
- $(f_{OS} + \Delta f_{vr})$ coefficient of wheel rolling resistance at the ground without applied torque (non-traction wheels)
 - λ tangential elasticity modulus of tires

To summarize, the power transmission efficiency coefficient η_{PL} for a transport unit is made up from the losses through the engine, drive train and wheels as given by:

$$\eta_{PL} = \eta_{EA} \cdot \eta_{DT} \cdot \eta_{TW}$$

To investigate these losses and identify how they can be minimized, each in turn must be broken down into their own individual components. Thus the coefficient of engine external power losses is comprised of the losses upon engine acceleration η_a , the losses related to the engine ambient temperature η_{EAT} , the losses owing to the height above sea level η_{SL} and the losses through the engine accessories η_{EC} (each accessory must be investigated separately).

The drive train efficiency coefficient η_{DT} is the product of the coefficient of losses in the transmission, universal joints, forward-rear axle and rear-rear axle with the transmission and axles each having an oil churning and mechanical friction component.

The efficiency at the wheels η_{TW} is how much of the torque applied on the wheels is translated into tractive force. This depends on the tire type, tire tread, tire inflation, tire load, tire temperature, torque applied to the wheel, road surface and the temperature of the road surface.

D.1.3. Engine performance ratings at full and partial load

An engine's performance ratings are represented by power, torque and fuel consumption curves as determined by engine velocity in RPM. These are used both to evaluate engine performance and to calculate the energy balance of a moving truck.

Later FERIC will study these engine ratings (and use them in duty cycle analysis) on a moving truck or on the truck test bench. We have already decided on and ordered the necessary instrumentation.

D.1.4. Power transmission ratings

The transmission parameters have a substantial impact on the properties of an automotive vehicle. The most important parameters are the drive ratios and their graduation, as well as the efficiency of the transmission and rear axles. The rear axle ratio is also a major factor in road performance.

The systematic analysis of the nature and effects of these factors will be part of the data collected during the study and analysis of logging truck duty cycles. The road vehicles in the study will be selected to cover a range of component designs and ratios.

D.1.5. Wheel radii

The no-load radius of a wheel r_{FR} (m) is specified by the manufacturer or determined by direct measurement on the truck (with the drive wheels elevated). Live radius (static) r_{LS} is specified by the manufacturer for a given load or else measured on the loaded truck. Kinematic radius r_{LK} and dynamic radius r_{LD}^M are:

$$r_{LK}^{\circ} = r_{FR} - 0.09 \cdot \sqrt{\frac{G_W}{p_w}} \quad (10)$$

and with applied torque

$$r_{LD}^M = r_{FR} - 0.09 \cdot \sqrt{\frac{G_W}{p_w}} - \frac{F_{TR}^2}{\sqrt{G_W \cdot p_w}} \quad (11)$$

where: - p_w is the inflation pressure of driving tires, daN/m²

Given the structure of the equations, the loaded radius r_{LD}^M is disregarded in tests with the wheels lifted off the ground. It is extremely important, however, in road testing for it determines the force of ground traction which the transmission system transmits from the engine.

D.1.6. Center of gravity coordinates

As was described in report TR-53, the locus of the center of gravity affects a vehicle's road performance. The duty cycle instrumentation has been designed to permit this relationship to be studied with the particular objective to understand the operating conditions under which loaded trucks can become unstable and subject to tipping or spilling their load.

D.1.7. Moments of inertia

The moments of inertia of rotating components must be included in any analysis of transport unit energy losses. The main ones are the moments of inertia of the tires with wheels, of the drive train and of the engine.

D.1.7.1. Moment of inertia of tire with wheel, J_{WT} (daN·m·sec²)

Report TR-53 gives the approximate empirical formula (18) for calculating the moment of inertia of a wheel. This formula was verified through tests based on the investigative method devised by R.F. Gonsalves of Canadian Pacific's research department. As shown in appendix J.0, there was very good correlation between the experimental result ($J_{WT} = 2.12$ daN·m·sec²) and that determined from the empirical formula ($J_{WT} = 2.13$ daN·m·sec²).

D.1.7.2. Moment of inertia of all driving tires with wheels, $J_{\Sigma WT}$ (daN·m·sec²)

This moment is established by multiplying the moment of one tire with wheel by the total number of driving tires.

D.1.7.3. Drive train (without wheels) moment of inertia J_{DT} (daN·m·sec²)

The moment of inertia of the drive train was measured for a lifted truck with wheels installed and with wheels removed. The results (without wheels) ranged between 0.85 and 1.00 daN·m·sec² which is about five percent of the moment of inertia of all driving wheels ($8 \times 2.13 = 17.04$ daN·m·sec²) and compares very favourably with the commonly accepted empirical factor referred to with formula (21) in TR-53.

D.1.8. Air resistance coefficient C_{FRO}

It is known from aerodynamics that the force of frontal resistance of a moving vehicle equals:

$$F_{AR} = C_{FRO} \cdot P_d \cdot S \quad (12)$$

- where: - F_{AR} force of frontal resistance of moving vehicle, daN
- C_{FRO} coefficient of frontal resistance
- P_d dynamic pressure on frontal area, daN/m²
- S maximum frontal area, m²

To take into account the influence of the Mach (Ma) and Reynolds (Re) numbers on coefficient C_{FRO} , equation (12) is written as:

$$F_{AR} = C_{FRO} \cdot \frac{\rho \cdot v_{AIR}^2}{2} \cdot S \quad (13)$$

- where: - ρ atmospheric pressure
 - v_{AIR} air velocity in m/sec.

We now come to the effect of the volumetric mass on the frontal resistance of air. Given that:

$$\gamma = \frac{10\ 333 \cdot \rho}{760\ RT} \quad (14)$$

or:

$$\gamma = g \cdot \rho \approx 13.6 \frac{\rho}{RT} \quad (15)$$

- where: - γ density of the air
 - R molar constant of gasses
 - T absolute temperature in $^{\circ}K$
 - g gravitational acceleration, m/sec^2

Equations (14) and (15) can be used to determine how the ambient temperature affects coefficient ρ .

This effect is illustrated in Figure 5 where it is seen that the volumetric mass of air increases by a factor of 1.25 over the $80^{\circ}C$ ambient temperature range encountered in central and eastern Canadian logging conditions. For this same temperature range, and using $288^{\circ}K$ ($15^{\circ}C$) as the normal reference temperature, air resistance is thus 20% higher at $-40^{\circ}C$ and 5% lower at $+40^{\circ}C$.

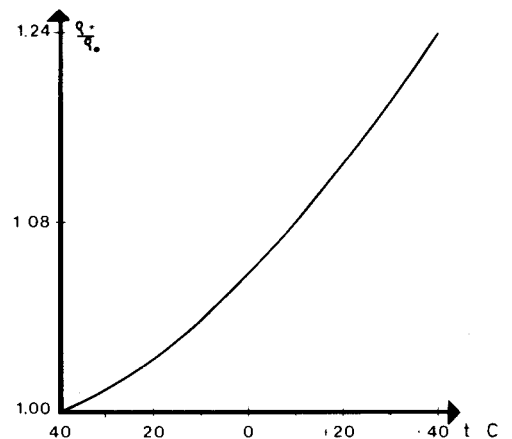


Figure 5 Effect of ambient temperature on air density coefficient ρ/ρ_0 .

* ρ_0 = volumetric mass of air in $daN \cdot s^2/m^4$ under the following atmospheric conditions ($\rho_0 = 0.125 daN \cdot s^2/m^4$):
 P (barometric pressure) = $10\ 132.48 daN/m^2$
 T₀ (ambient temperature) = $288^{\circ}K$

The air resistance coefficient C_{FRO} is calculated using coefficient K procedure of which determination has been given in the report TR-53. As

$$C_{FRO} = \frac{2 \cdot K}{\rho} \quad (16)$$

C_{FRO} can be found for a given ρ based on atmospheric conditions. Practically speaking, at 60 km/h, a 30% difference in air resistance represents a difference of roughly 10 hp or about 0.70 kg/h in fuel consumption.

D.1.9. Rolling resistance coefficient f_{RR}

The rolling resistance is affected by the road vertical and horizontal profile, its surface smoothness and its distortion under load. It is also influenced by some features in the vehicle design such as the camber of the front steering wheels, the angle of lateral slip of the front wheels, the vibratory response of the suspension system (tires and springs) to the inconsistencies of the road surface and, finally, the torque applied to the drive wheels is an important factor. The FERIC project has been designed to study each of these variables using the methodology as developed in the following equations.

Coefficient f_{RR} can be written out fully as follows:

$$f_{RR} = [(f_{OS} + \Delta f_{v_r})^* + \Delta f_M + \Delta f_{\delta} + \Delta f_C + \Delta f_{GD} + \Delta f_{ur}] \cdot \cos \alpha + \sin \alpha \quad (17)$$

- where:
- α angle of vertical gradient of road, in degrees
 - f_{OS} coefficient of rolling resistance at low speeds ($\frac{P_{f\Sigma}^{\circ}}{G_T} = f_{OS}$)
 - Δf_{v_r} increment of coefficient f_{OS} through increase in road speed
 $(\Delta f_{v_r} = \frac{k \cdot v_r^2}{G_T})$
 - Δf_M increment of coefficient f_{OS} through application of torque to the drive wheels; this increment is calculated by the following formula:

$$\Delta f_M = \frac{F_{TR} \cdot (r_{LK}^{\circ} - r_{LD}^M)}{G_T \cdot r_{LK}^{\circ}} \quad (18)$$

* This coefficient is given as $(\frac{P_{f\Sigma}^{\circ} + k \cdot v_r^2}{G_T})$ in report TR-53.

With ISO symbols which will be used in this and future reports

$$\frac{P_{f\Sigma}^{\circ}}{G_T} = f_{OS}; \text{ and } \frac{k \cdot v_r^2}{G_T} = \Delta f_{v_r}$$

where: - F_{TR} total resisting force of driving tires on the ground (including air and rolling resistances at a given speed) in daN

The force F_{TR} and the total vehicle weight G_T have been determined by field tests and radii are calculated by equations (10) and (11).

- Δf_C increment of coefficient f_{OS} by resistance through camber of front (steering) wheels. $\Delta f_C = C_{CR} \cdot \beta$ where β is the camber and C_{CR} the coefficient of resistance as determined by the camber
- Δf_δ increment of coefficient f_{OS} by resistance through angle of side slip of front (steering) wheels. $\Delta f_\delta = C_{SS} (\beta \cdot \delta + \delta^2)$ where δ is the side slip angle and C_{SS} the coefficient of resistance due to side slip.

These additions to coefficient f_{OS} will be examined during duty cycle testing of a road vehicle.

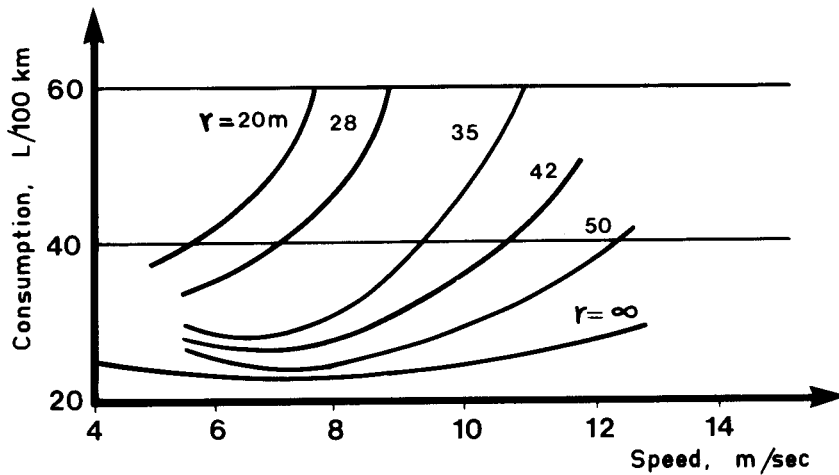


Figure 6: Effect of road curve radii on fuel consumption.

Figure 6 illustrates the importance of road curvature relative to power consumption. As is seen from this figure, power consumption-- and thus the coefficient-- may triple for a pronounced curve as compared to a straight path.

- Δf_{GD} increment of coefficient f_{OS} through that part of resistance caused by ground distorsion. Δf_{GD} can be determined by empirical formula.

$$\Delta f_{GD} = \frac{0.12}{C_{SD}} + 0.05 \quad (19)$$

where: - C_{SD} coefficient caused by ground distorsion resistance. This factor will be examined in future duty cycle testing on ground subject to deformation.

- Δf_{SV} increment of coefficient f_{OS} through vibration in the suspension (tires and springs) of road vehicle. This component of the rolling resistance coefficient will also be studied during duty cycle testing.

- Δf_{ur} increment of coefficient f_{OS} through unevenness of road surface. This component is given by the following equation:

$$\Delta f_{ur} = C_{UC} \cdot d_{rs} \cdot v_r^2 \cdot 10^{-9} \quad (20)$$

where: - C_{UC} undercarriage coefficient (normally 5.5 for trucks)

- d_{rs} road surface dispersal, cm/km

- v_r road speed, m/sec

All of these coefficients as well as other factors may enter into our future studies. Each analysis of our operating conditions provides an opportunity to enhance the work environment and thereby reduce power consumption and improve machine durability and road performance.

D.2 TRACTIVE EFFORT F_T (daN)

The tractive effort available to move a transport unit at the selected speed depends on the force available at the engine output multiplied by transmission and rear axle ratios and reduced by the losses imposed by the drive train.

Vehicle movement on the road requires that tractive effort to overcome all resistances. Figure 7 gives schematically what happens when the engine output torque multiplied by transmission and rear axle ratios minus drivelines losses is applied on a driving wheel.

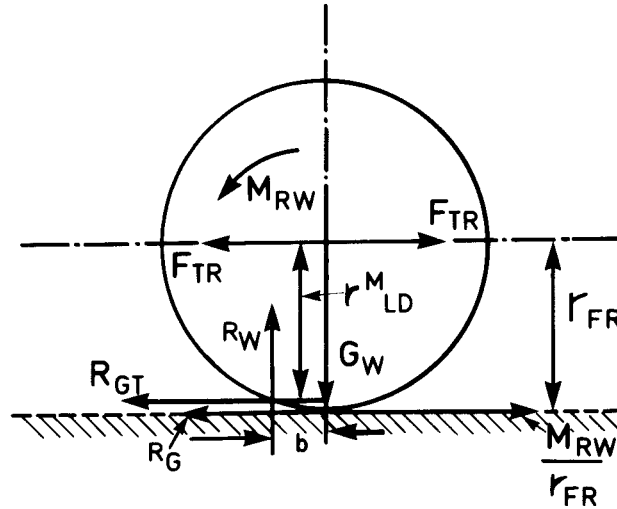


Figure 7: Ground balance of traction wheel.

Equation (21) yields this tangential reaction.

$$R_G = \frac{M_{RW}}{r_{FR}} - F_{TR} \quad (21)$$

and:

$$R_{GT} = \frac{M_{RW}}{r_{LD}^M} - F_{TR} \quad (22)$$

- where:
- R_G reaction at the ground, daN
 - M_{RW} rotating moment of wheels, daN·m
 - r_{FR} free radius of tires, m
 - r_{LD}^M dynamic radius of tires, m
 - F_{TR} total force of rolling resistance, daN
(traction without slip)
 - R_{GT} reaction at the ground (with applied torque), daN
 - b resisting moment lever, m

Expression M_{RW}/r_{FR} represents the circumferential effort on the tires of the drive wheels without slip at the point of ground contact while M_{RW}/r_{LD}^M is the circumferential effort as modified by the radius distortion because of the torque application on wheels.

The moment of rotation of the drive wheels is known to equal:

$$M_{RW} = M_{EV} \cdot i_{TR} \cdot i_{RA} \cdot \eta_{DT} \quad (23)$$

- where:
- M_{EV} moment at engine output, daN·m
 - i_{TR} drive transmission ratio
 - i_{RA} rear axle ratio
 - η_{DT} overall drive train efficiency

The engine moment of rotation M_{EV} is a variable dependent on the position of the accelerator pedal (chosen by the driver) as determined by his perceived need for the road performance desired. Figure 8 diagrams two situations in which the driver chooses the torque required for the service conditions at hand.

At point A the pedal is pressed down 10° to maintain velocity v_r' with a moment of resistance of $(M_R^r)'$. At point B the angle of depression is 30° to meet the demand in moment $(M_R^r)''$ at velocity v_r'' .

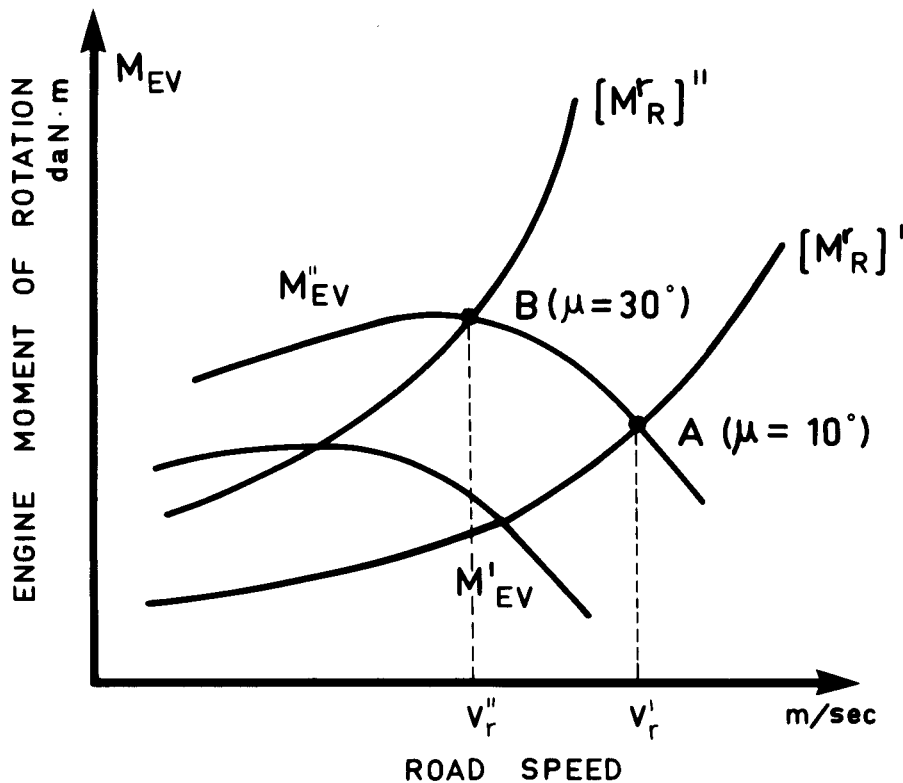


Figure 8: Example of standard utilization of engine torque.

This clearly illustrates the interplay between the human factor (driver), the vehicle and the road. By measuring the deflection of the accelerator pedal from its original position and the engine torque for a given speed, as well as knowing the drive and rear axle ratios and drive train losses, we can at any moment relate this equilibrium to the actual operating conditions of a road vehicle.

Moment M_{EV} , which is measured at variable engine velocity, is composed of the moment M_{ES} corresponding to the same but stabilized velocity and the force of inertia. This gives:

$$M_{EV} = M_{ES} + J_E \cdot \frac{d\omega_{EN}}{dt} \quad (24)$$

- where:
- M_{EV} engine moment of rotation at variable velocity (deceleration or acceleration), daN·m
 - M_{ES} engine moment of rotation at steady velocity, daN·m
 - J_E overall moment of inertia of engine (including engine flywheel), daN·m·sec²
 - ω_{EN} engine angular velocity, sec⁻¹ ($n \cdot \pi / 30$)
 - t time, sec

This moment M_{EV} has to be transmitted to the driving wheels. On transmitting it to wheels it has to be multiplied by the transmission ratio and again multiplied by the rear axle ratio. On the other hand it is reduced by the drive train oil churning and friction losses and therefore has to be multiplied by the drive train efficiency. To obtain the traction force on driving wheels it has also to be divided by the dynamic radius. Following equation expresses this transformation:

$$F_T = (M_{ES} + J_E \cdot \frac{d\omega_{EN}}{dt}) \cdot \frac{i_{TR} \cdot i_{RA}}{r_{LD}} \cdot \eta_{DT} \quad (25)$$

- where:
- F_T is the tractive force
 - i_{TR} is the transmission ratio
 - i_{RA} is the rear axle ratio
 - η_{DT} is the drive train efficiency coefficient

When there is no tire slip on the ground, the angular velocity of the motor can be written

$$\omega_{EN} = \frac{v_r}{r_M} \cdot i_{TR} \cdot i_{RA} \quad (26)$$

and finally, the total tractive force needed to move the vehicle at the selected speed is given by the force to move it at a steady velocity plus or minus the moment of inertia of the engine and drive train, depending upon whether the engine is accelerating or decelerating at that time. Thus

$$F_T = F_{ST} \pm J_E \left(\frac{i_{TR} \cdot i_{RA}^2}{r_{LD}} \right) \cdot \eta_{DT} \cdot \frac{dv_r}{dt} \quad (27)$$

where: - F_{ST} effort at the drive wheels at steady velocity; this effort is equal to:

$$F_{ST} = M_{ES} \frac{i_{TR} \cdot i_{RA}}{r_{LD}} \cdot \eta_{DT} \quad (28)$$

The sign (-) designates engine acceleration whereas (+) designates engine deceleration.

The maximum value of tractive effort is limited by tire slip on the ground. Tire gripping power F_{SA} is equal to:

$$F_{SA} = R_{GW} \cdot \phi \quad (29)$$

where: - R_{GW} reaction at the ground to the weight on wheel, daN
 - ϕ coefficient of tire grip on the ground

Naturally, effort F_T must be less than or equal to effort F_{SA} . Otherwise, slipping will occur. In other words,

$$F_T \leq R_{GW} \cdot (\phi + f_{RR}) \quad (30)$$

If we have $F_T > R_{GW} \cdot (\phi + f_{RR})$, corresponding to the slipping conditions, only that portion of traction corresponding to the total force of resistance at the ground, plus the force of adhesion, will be developed at the wheels. The excess applied force available is just used in spinning the wheels.

D.2.1.1. Forces of resistance related to the drive train and wheel bearings friction

The forces of drive train resistance are contingent on several factors, e.g.:

- transmitted torque;
- velocity;
- oil temperatures;
- oil types;
- component design, etc...

According to the results presented further on, these resistances vary linearly as a function of speed. Thus:

$$F_{DTR} = F_{OUT} (1 - \eta_{FR}) + F_{OC} \quad (31)$$

or:

$$F_{DTR} = F_{OUT} (1 - \eta_{DT}) \quad (32)$$

- where:
- F_{DTR} force of drive train resistance, daN
 - F_{OUT} engine output force, daN
 - F_{OC} force of resistance of the oil to churning
 - η_{DT} overall drive train efficiency coefficient
 - η_{FR} drive train friction efficiency coefficient

The first member of equation (31) represents the losses through transmitted power and the second the losses through oil churning (in daN).

The forces of resistance through friction in the non-drive wheel bearings can be determined by the coast down method described in report TR-53. This means elevating one wheel and determining deceleration j_{WT} in m/sec^2 . The equation for deriving this force is as follows:

$$F_{rr} = \frac{Z_w \cdot J_{WT} \cdot j_{WT}}{r_{LK}} \quad (33)$$

- where:
- F_{rr} force of resistance in bearings of all non-drive wheels, daN
 - Z_w number of wheels

- J_{WT} moment of inertia of one wheel, $\text{daN}\cdot\text{m}\cdot\text{sec}^2$
- j_{WT} wheel deceleration, m/sec^2
- r_{LK}° kinematic radius, m

D.2.2. Force of rolling resistance F_{RR}

The force of rolling resistance F_{RR} is dependent upon the total vehicle mass and the rolling resistance of the vehicle within the environment in which it is being used. It can generally be written as:

$$F_{RR} = G_T \cdot f_{RR} \quad (34)$$

where: - G_T total vehicle mass in kg.

Using equation (17) for the rolling resistance coefficient f_{RR} , we obtain:

$$F_{RR} = \{ [(f_{OS} + \Delta f_{vr}) + \Delta f_M + \Delta f_{\delta} + \Delta f_C + \Delta f_{GD} + \Delta f_{SV} + \Delta f_{ur}] \cos\alpha + \sin\alpha \} \cdot G_T \quad (35)$$

D.2.3. Force of air resistance F_{AR}

This force is calculated as indicated by the formula (13) modified by the equation (16):

$$F_{AR} = K \cdot v_{AIR}^2 \cdot S \quad (36)$$

D.2.4. Inertia forces F_I

The variables influencing the inertia forces are the vehicle mass and its acceleration according to the formula:

$$F_I = m_T \cdot J_a \quad (37)$$

where: - m_T total mass of loaded vehicle $\left(\frac{G_T}{g}\right)$
 - J_a vehicle acceleration, m/sec^2

D.3. EQUATION OF A MOVING VEHICLE (DUTY CYCLE EQUATION)

To write the general equation for a moving vehicle, let us look at the effect of the reactions attributable to the external forces acting on a truck-trailer (considered as a single mass concentrated at its center of gravity). First of all the ground tractive effort should be established. The equation (27) for this was developed in section D.2 and was given as:

$$F_T = F_{ST}(v_r) \pm J_E \left(\frac{i_{TR} \cdot i_{RA}}{r_M} \right)^2 \cdot \eta_{DT} \cdot \frac{dv_r}{dt}$$

Several resisting forces are acting against the tractive force. In order to have a tractive force equilibrium at any point on the road, the sum of all the forces is expressed as :

$$F_T + F_{AR} + F_I + F_{ir} + F_{RR} + F_{OC} = 0 \quad (38)$$

where: - F_{AR} is the air resisting force in daN (see equations 13 and 16) and $F_{AR} = \cdot K \cdot S \cdot v_r^2$

- F_I is the inertia force (see equation 37) and

$$F_I = m_T \cdot J_a \quad \text{and} \quad F_I = m_T \cdot \frac{dv_r}{dt}$$

- F_{RR} is the rolling resistance force and

$$F_{RR} = G_T (f_{RR} \cos \alpha \pm \sin \alpha)$$

- F_{ir} is the inertia force of rotating wheels and drivetrain and

$$F_{ir} = \frac{(\sum J_{WT} + J_{DT})}{(r_{LD}^M)^2} \cdot \frac{dv_r}{dt}$$

- F_{OC}^* is the force corresponding to oil churning losses, daN

The tractive force equilibrium diagram is illustrated in Figure 9.

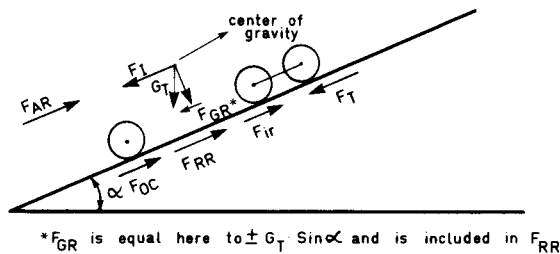


Figure 9 : Tractive forces road equilibrium diagram.

* F_{OC} is equal to P_{tp}° force in TR-53 report.

Equation 38 can be written

$$F_{ST}(v_r) + J_E \left(\frac{i_{TR} \cdot i_{RA}}{r_{LD}^M} \right)^2 \cdot \eta_{DT} \cdot \frac{dv_r}{dt} + K \cdot S \cdot v_r^2 + \frac{(\sum J_{WT} + J_{DT})}{(r_{LD}^M)^2} \cdot \frac{dv_r}{dt} + m_T^* \cdot \frac{dv_r}{dt} + G_T (f_{RR} \cos \alpha \pm \sin \alpha) + F_{OC} = 0 \quad (39)$$

and:

$$[m_T + J_E \cdot \left(\frac{i_{TR} \cdot i_{RA}}{r_{LD}^M} \right)^2 \cdot \eta_{DT} + (\sum J_{WT} + J_{DT}) \cdot (r_{LD}^M)^{-2}] \cdot \frac{dv_r}{dt} + K \cdot S \cdot v_r^2 + F_{ST}(v_r) + G_T \cdot (f_{RR} \cdot \cos \alpha \pm \sin \alpha) + F_{OC} = 0 \quad (40)$$

Portion of this equation written between brackets [] is equal to:

$$m_T + J_E \cdot \left(\frac{i_{TR} \cdot i_{RA}}{r_{LD}^M} \right)^2 \cdot \eta_{DT} + (\sum J_{WT} + J_{DT}) \cdot (r_{LD}^M)^{-2} = m_T \cdot \delta_{RM} \quad (41)$$

and dividing the whole by m_T , the following coefficient is obtained:

$$\delta_{RM} = 1 + \frac{J_E}{m_T} \cdot \left(\frac{i_{TR} \cdot i_{RA}}{r_{LD}^M} \right)^2 \cdot \eta_{DT} + \frac{(\sum J_{WT} + J_{DT}) \cdot (r_{LD}^M)^{-2}}{G_T} \quad (42)$$

The coefficient δ_{RM} takes account of all the rotating masses of the vehicle.

In the equation (40) the expression between brackets is replaced by $m_T \delta_{RM}$ and the whole divided by G_T , expression that encompasses all the forces in balance of a moving vehicle at any given moment becomes

$$\frac{\delta_{RM}}{g} \cdot \frac{dv_r}{dt} \pm \frac{F_{ST}(v_r) \pm K \cdot S \cdot v_r^2 + F_{OC}}{G_T} + \psi = 0 \quad (44)$$

We now turn to the different situations that may occur on the road.

* here $m_T = \frac{G_T}{g}$

1) Traction

In this case, the tractive effort $F_{TS}(v_r) > 0$, giving the relationship

$$\frac{\delta_{RM}}{g} \cdot \frac{dv_r}{dt} - \frac{F_{ST}(v_r) - K \cdot S \cdot v_r^2 + F_{OC}}{G_T} + \psi = 0 \quad (45)$$

2) Free wheeling

With free wheeling, the traction effort $F_{ST}(v_r) = 0$ and, as the engine is disconnected from the drive train

$$J_E \cdot \left(\frac{i_{TR} \cdot i_{RA}}{r_{LD}^M} \right)^2 \cdot \eta_{DT} = 0$$

Then, first:

$$\delta'_{RM} = 1 + \frac{(\sum J_{WT} + J_{DT}) \cdot g}{G_T (r_{LD}^M)^2} \quad (46)$$

and:

$$\frac{\delta'_{RM}}{g} \cdot \frac{dv_r}{dt} + \frac{K \cdot S \cdot v_r^2 + F_{OC}}{G_T} + \psi = 0 \quad (47)$$

3) Braking

There are two possibilities here:

(a) Braking with the engine isolated from the power transmission system when

$$\frac{\delta'_{RM}}{g} \cdot \frac{dv_r}{dt} + \frac{F_{MBR}(v_r) + K \cdot S \cdot v_r^2 + F_{OC}}{G_T} + \psi = 0 \quad (48)$$

(b) Braking by using the engine and the main braking system, then

$$\frac{\delta'_{RM}}{g} \cdot \frac{dv_r}{dt} + \frac{F_{BEF}(v_r) + K \cdot S \cdot v_r^2 + F_{OC}}{G_T} + \psi = 0 \quad (49)$$

where: braking effort $F_{BEF}(v_r) = F_{MBR} + M_{EBR} \cdot \frac{i_{TR} i_{RA}}{r_{LD} M} \cdot \eta_{DT}$

with

F_{MBR} being the braking effort of the main braking system in daN

M_{EBR} being the braking moment of the engine in daN·m

4) Travel state

What is more, the vehicle runs in one of three states:

- acceleration when $\frac{dv_r}{dt} > 0$
- steady speed when $\frac{dv_r}{dt} = 0$
- deceleration when $\frac{dv_r}{dt} < 0$

Why have these equations been developed and included in the body of this report? The purpose of the FERIC program is to improve the efficiency of the forestry transport operations. Examination of the equations identifies the most important variables which can be changed to have a positive or negative effect on the transport costs. These include:

- average transmission ratio (determined by specifying the transmission ratio, selecting the engine size and driver performance);
- rear axle ratio (during specification of unit);
- transmission and drive axle losses from oil churning (viscosity and temperature of oils during use) and mechanical friction (oil selection, gear design and applied torque);
- tire inflation and size;
- road - curves
 - grades
 - surface;
- load size;
- average road speed (determined by driver performance, rolling resistance, air resistance and load for any given transport unit);
- air resistance (vehicle and load configuration).

If we are able to establish the factors influencing the driver-vehicle-operation relationship (and their magnitude), these equations of typical situations can be used to analyse the vehicle and operator performance at any point along the road. Practical actions to improve the performance of existing transport operations can be identified. Also, knowledge will be gained which can be used to specify more efficient transport units for the existing conditions when replacement units are being selected.

E. SAMPLE ENERGY BALANCE FOR A ROAD VEHICLE

Figures 10-12 chart three energy balances for the same vehicle and roughly the same mass of 60 000 kg at a steady speed of 56 km/h but on different road surfaces and, for the winter test, at a different ambient temperature.

Figure 10 gives the results obtained on an asphalt road during the summer months at an ambient temperature of +32°C. The same truck was tested almost simultaneously on a hard, dry gravel road at the same ambient temperature (Figure 11). It was later tested in winter on a snow-covered icy gravel road featuring a hard smooth surface (Figure 12) at an ambient temperature of -32°C.

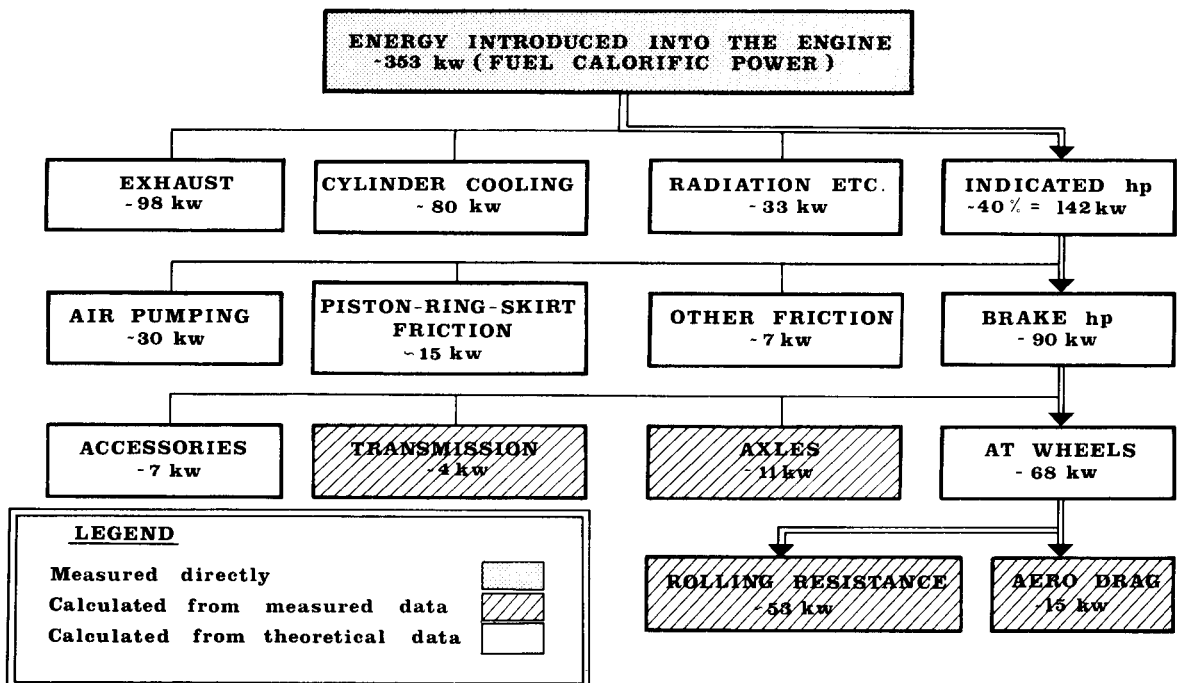


Figure 10 : Energy balance on a straight paved road (G.C.W. 60 000 kg steady speed of 56 km/h, direct drive, summer conditions dry & +32°C).

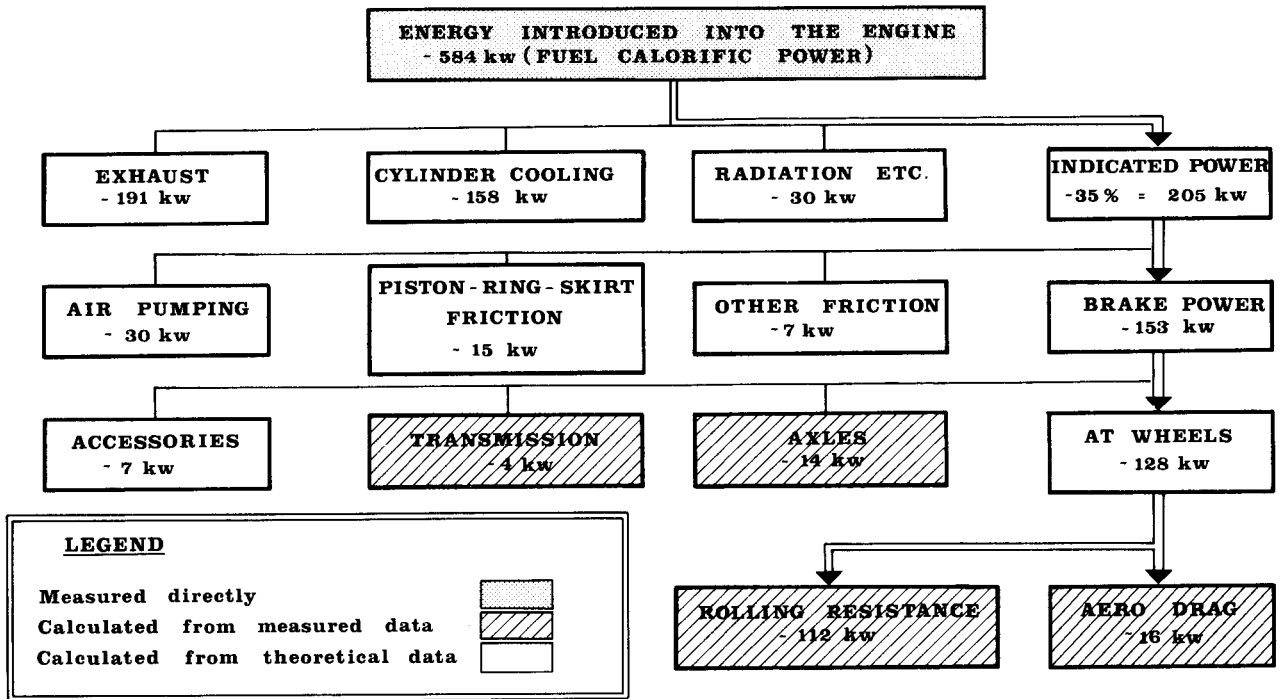


Figure 11: Energy balance on a straight, flat gravel road [summer]

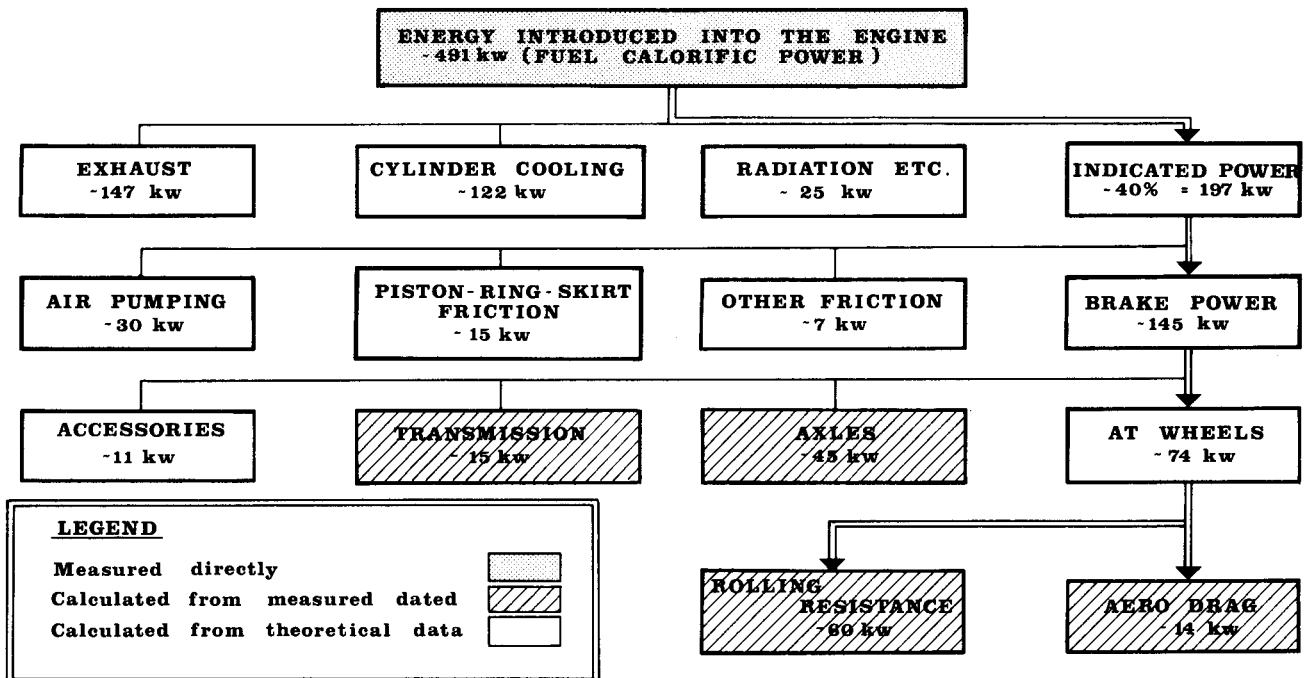


Figure 12: Truck energy balance on a snow-covered icy gravel road.

It is readily seen that power consumption on a gravel road is considerably higher than on an asphalt road in the summer. In the winter, the rolling resistance of the hard, smooth, icy surface of the gravel road approached that of the asphalt road in the summer. However the power savings were negated by much higher losses in the power transmission system because of the effect of the lower oil temperatures (higher oil viscosities).

This type of analysis (duty cycle or energy balance) can therefore be used to determine the factors affecting power consumption and performance. In addition, through several repetitions of this type of investigation and variation of the factors, it can serve to optimize the elements of our transport operations.

F. COMMENTS ON COMPONENT LUBRICATION THEORY AND THE EXPERIMENTAL RESULTS FROM AN INVESTIGATION OF DRIVE TRAIN POWER LOSSES

F.0 COMMENTS ON COMPONENT LUBRICATION THEORY

The findings described below concern the power losses owing to problems of lubrication of the gears and traction axles of road trucks. There are two causes for these power losses, oil churning and mechanical friction.

(a) Oil churning

- It is well known that churning losses depend largely on the viscosity of the oil at a given temperature (see results further on).
- Oil churning losses also depend on the rotating velocity of the power transmission system.

(b) Mechanical friction

- Mechanical friction is a function of the viscosity of the oils used. Studies have shown such losses declining with a reduction in viscosity (in a hydrodynamic state).
- It generally diminishes as the temperature rises but there can be a point related to applied torque beyond which the mechanical friction can increase.
- It is a function of the type of oil and oil additives involved, (e.g. antifriction additives).

F.1 EXPERIMENTAL RESULTS REGARDING DRIVE TRAIN POWER LOSSES

F.1.0. Verification of the methodology and accuracy of resistance determinations and consumption measurements

As was discussed in report TR-53, the forces of resistance owing to oil churning in the transmissions and rear drive axles, F_{OC} , are determined by the coast down method^①. Given the method's complexity and even more the potential for instrument or human error, one of the first tasks was to verify the accuracy of the results.

Two types of instruments were used for the verification^②. The measurements, although basically different in view of the principle involved, evaluate the same quantities by different methods. The evaluation covers the forces of resistance on the one hand and the energy consumption corresponding to those forces on the other, making it possible to compare results derived by entirely different methods.

Table 1 gives the results for fuel consumption measurements converted to forces of resistance, compared to the resistance forces calculated by the coast down method. The differences range between 0.1 and 2.9%, for an average of 1.27%. These comparisons point up the acceptable accuracy and reliability of both the resistance calculation procedure and the power consumption measurements. These comparative results were obtained through the use of a FERIC devised fuel measurement system based on fuel weight which is accurate to within 0.1 g^③.

Once it has been ascertained that the system of analysis is reliable, it is a matter of investigating the factors affecting the magnitude of the resistance caused by oil churning in the transmissions and rear axles.

F.1.1. Operating factors affecting resistance forces

F.1.1.0 Road speed

It was recognized in report TR-53 that the forces of resistance through oil churning are comprised of an initial force at near zero speeds and an addition that increments linearly with speed. This can be written as:

$$F_{OC}^{③} = (F_{OC}^{\circ})^{④} + a \cdot v_r \quad (50)$$

① In report TR-53 resistances through oil churning are designated P_{tp}° .

② See description in the appendix.

③ P_{tp}° in report TR-53.

④ $P_{tp_o}^{\circ}$ in report TR-53.

A) STANDARD OIL

TEST DATE	TEST NUMBER	DRIVE TRAIN RATIOS	number of accumulated revolutions measured	loaded tire radius at test speed	coeff of reciprocity	CONSUMPTION MEASURED AT TEST TEMPERATURE			Q _{TA} ②	R _{OCC} ③	resistance calculated by coast down method	percent difference
						TRANSM	F-R AXLE	R-R AXLE				
—	—	λ	n	m	—	°C kg/h	°C kg/h	°C kg/h	kg/h	daN	daN	%
March 1, 1983	18	5.9	3600	0.532	0.0000032829	70 0.39	60 0.53	56.4 0.39	1.31	41.00	41.83	—
-II-	2	-II-	-II-	-II-	-II-	52.7 0.51	61.1 0.53	11.6 1.32	2.36	73.81	74.17	0.5
-II-	11	-II-	-II-	-II-	-II-	71.6 0.39	62.5 0.51	40.6 0.55	1.45	45.36	45.42	0.1
-II-	14	-II-	-II-	-II-	-II-	67 0.41	59.4 0.54	47.5 0.47	1.42	44.42	45.66	2.7
II	7	-II-	-II-	-II-	-II-	60.8 0.45	59.7 0.54	26.5 0.81	1.80	56.30	56.84	1

B) SYNTHETIC OIL 'A'

March 15, 1983	8	5.9	3600	0.532	0.0000032829	74 0.27	73.5 0.45	8 1.05	1.73	54.11	53.60	1
----------------	---	-----	------	-------	--------------	------------	--------------	-----------	------	-------	-------	---

C) SYNTHETIC OIL 'B'

March 20, 1983	2	5.9	3600	0.532	0.0000032829	70.3 0.26	75.2 0.55	13 1.0	1.81	56.61	57.50	1.5
-II-	5	-II-	-II-	-II-	-II-	67.8 0.27	76.4 0.53	30.3 0.70	1.50	46.92	47.37	1
-II-	9	-II-	-II-	-II-	-II-	68.5 0.40	76 0.53	40 0.53	1.46	45.67	45.97	0.7
-II-	15	-II-	-II-	-II-	-II-	69.5 0.39	76.6 0.52	59.8 0.42	1.33	41.60	42.88	2.9

- ① Resistance and consumption values are given at 1,800 RPM.
- ② Fuel consumption related to transmission and axle oil churning losses.
- ③ Resistance calculated from fuel consumption.

TABLE 1: Comparison of power losses in the transmission and drive axles of a logging truck as calculated from fuel consumption measurements and by the coast down method (for three different lubricating oils) ①

where:

- F_{OC}° force of resistance through oil churning at near zero speeds, daN
- a coefficient for the rate of increase of drive train losses as a function of increase in speed, daN·sec/m
- v_r road speed, m/sec

This hypothesis was verified by a series of tests on the combined engine and drive of a truck with the drive wheels lifted off the ground. The fictive road speed was changed and the fuel consumption rate measured at each speed. Figure 13 gives these fuel consumption values converted to resistance forces related to road speed in m/sec. The results fully bear out the hypothesis of linear increase of the forces of resistance through oil churning. The tests were performed twice, once with the rear wheels installed and once without them. Figure 13 indicates very little resistance attributable to air churning by the wheels.

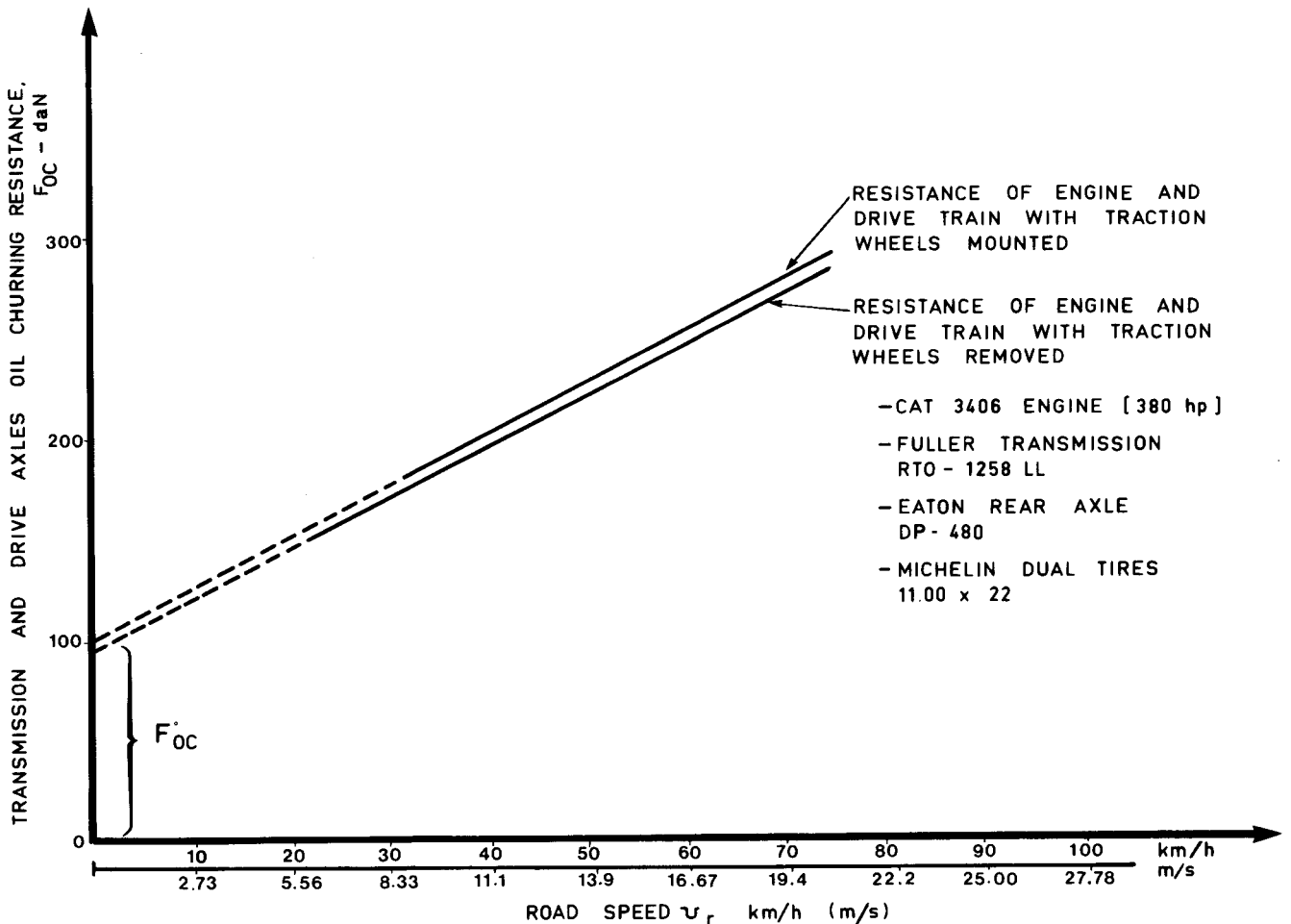


Figure 13 : Diagram of oil churning resistance to engine and drive train rotation (drive wheels lifted off the ground).

F.1.1.1.1. Oil temperatures (°C)

Having verified the accuracy of the investigations and the linearity of the increase in resistance in terms of road speed, we then examined how temperature affects the oil churning resistances. Given that the effect of temperatures on resistance cannot be investigated under actual operating conditions, which are necessarily variable, it was necessary to devise an electrical system for oil preheating and heating with hot engine coolant*. Special heat exchangers featuring thermo-controlled valves were employed and the desired constant oil temperature was imposed.

We started by testing only the transmission, then the transmission together with the forward-rear axle and finally the transmission and both axles. Through this procedure we deduced to what extent the resistances (fuel consumptions) are determined by the oil temperature in each individual component.

The test temperature range was +10°C to +70°C. After mathematically establishing the precise equations for these curves, we extrapolated the curves from +10°C to -50°C and from +70°C to +80°C. This procedure covered the full range of conditions that may materialize in the Canadian forestry industry.

Standard oil

Figure 14 gives individual fuel consumptions and oil churning resistances in terms of oil temperatures for the transmission, forward-rear axle and rear-rear axle. We used what is called "standard" oil.

This diagram elicits a number of comments.

- 1) Resistances (fuel consumptions) are extremely high at low temperatures. At -50°C the overall fuel consumption for the three components lubricated with standard oil is roughly 24.75 kg/h (see Figure 15). Matching this value against maximum fuel consumption for a vehicle having 60,000 kg total gross mass and traveling at 56 km/h--which represents about 21 kg/h--shows the tremendous power consumption required simply to churn the oil in the transmission and rear axles at this temperature.
- 2) The forward-rear axle displays the highest resistance, followed by the rear-rear axle and then the transmission.

* See description in the appendix.

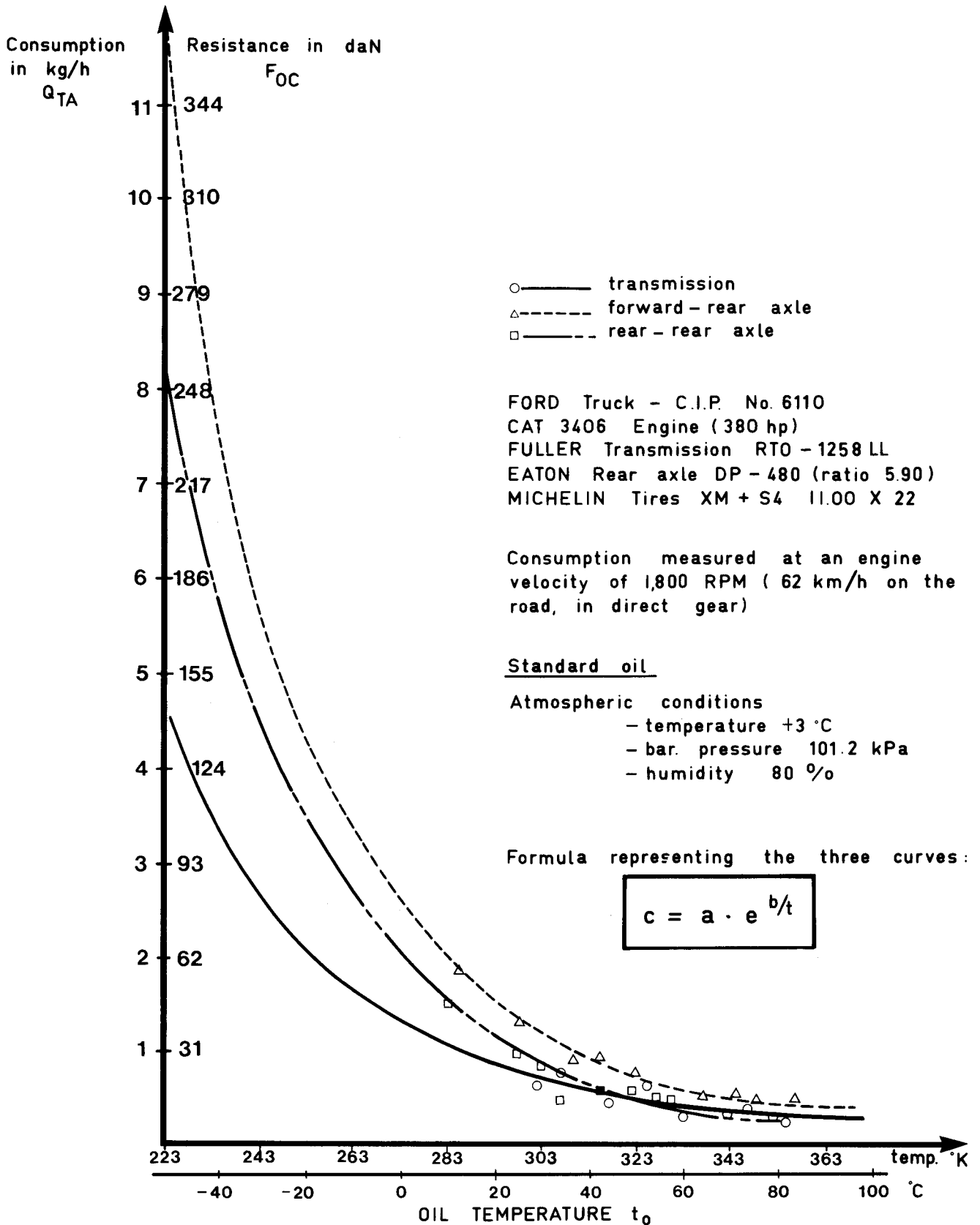


Figure 14 : Diagram of fuel consumption for standard oil.

- 3) At high temperatures the oil churning resistances of the transmission are higher than those of the rear-rear axle, whereas at low temperatures the resistances of the rear-rear axle oil are considerably higher than those of the transmission. This probably stems from the fact that as the oil liquefies and loses its lubricating film, it causes a more rapid increase in friction in the transmission than in the axle. The logical conclusion is that different oils should be used in the transmissions than in the rear axles, particularly in view of the different oils' properties at high temperatures.
- 4) As the mean operating temperatures were measured to be about 35°C in winter and 60°C in summer, the respective differences in resistance or fuel consumption at these temperatures and at the ideal oil temperature of some 80°C in relation to the vehicle total average fuel consumption on the road (roughly 21 kg/h for a mean speed of 56 km/h) can be calculated to be:

$$(a) \quad \% \text{ difference in winter } (35^{\circ}\text{C} - 80^{\circ}\text{C}) = \frac{2.48-1.00}{21 \text{ kg/h}}$$

$$\underline{\% \text{ difference in winter } (35^{\circ}\text{C} - 80^{\circ}\text{C}) = 7.00\%}$$

$$(b) \quad \% \text{ difference in summer} = \frac{1.62-1.35}{21}$$

$$\underline{\% \text{ difference in summer } (60^{\circ}\text{C} - 80^{\circ}\text{C}) = 1.29\%}$$

These figures highlight the importance of power transmission oil temperatures on fuel consumption and indicate the need to develop a practical lubricating oil heating system.

Figures 16 and 17 are diagrams that can be used to determine and add up the resistance forces, or fuel consumptions, for each individual component and then to determine, as a function of engine output power, the efficiency of the power transmission system. These diagrams are based on a mean engine velocity of 1,800 RPM. Naturally, the resistance or consumption values will change for a different engine velocity.

The industry can use these diagrams as working documents. Knowing the transmission, forward-rear and rear-rear axle oil temperatures, it can determine the losses for the three test oils (see Figures 16 and 17) by dividing the indicated fuel consumption by the total consumption in kg/h under operating conditions. Examples on how to use these graphs are given in section G.

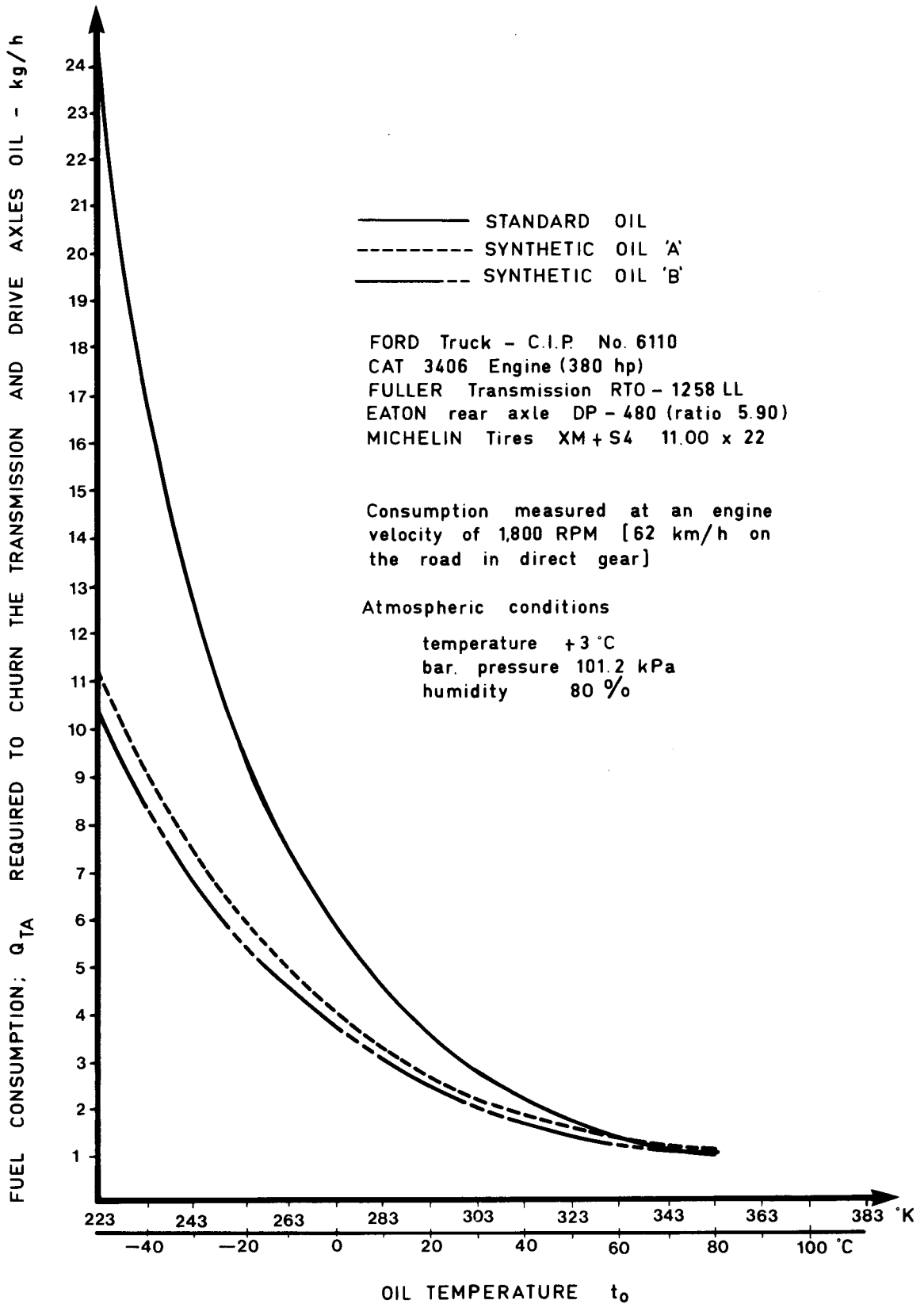


Figure 15 : Diagram of fuel consumption in terms of oil temperatures (transmission and two axles combined). Comparison of the three test oils.

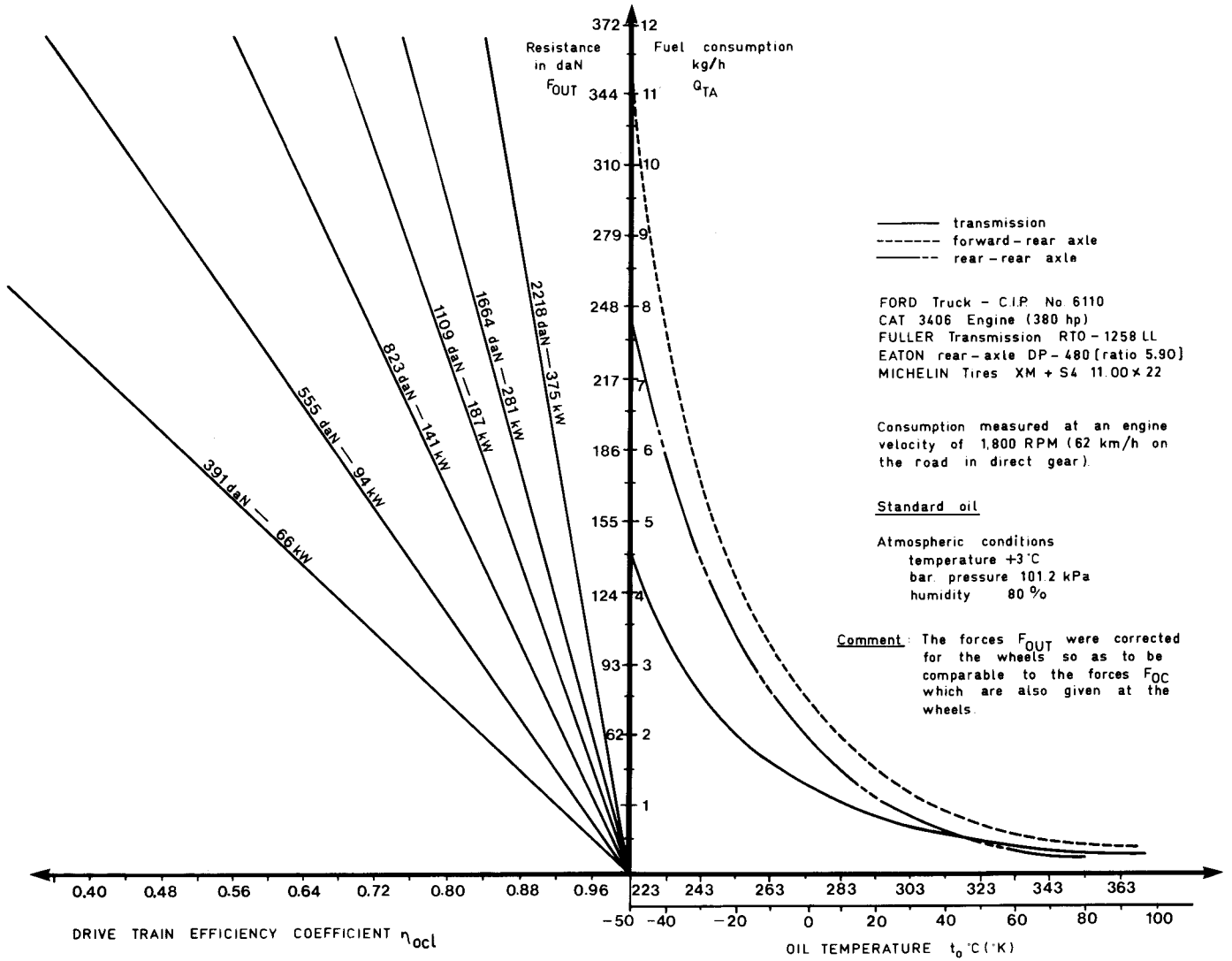


Figure 16: Establishment of drive train efficiency coefficients.

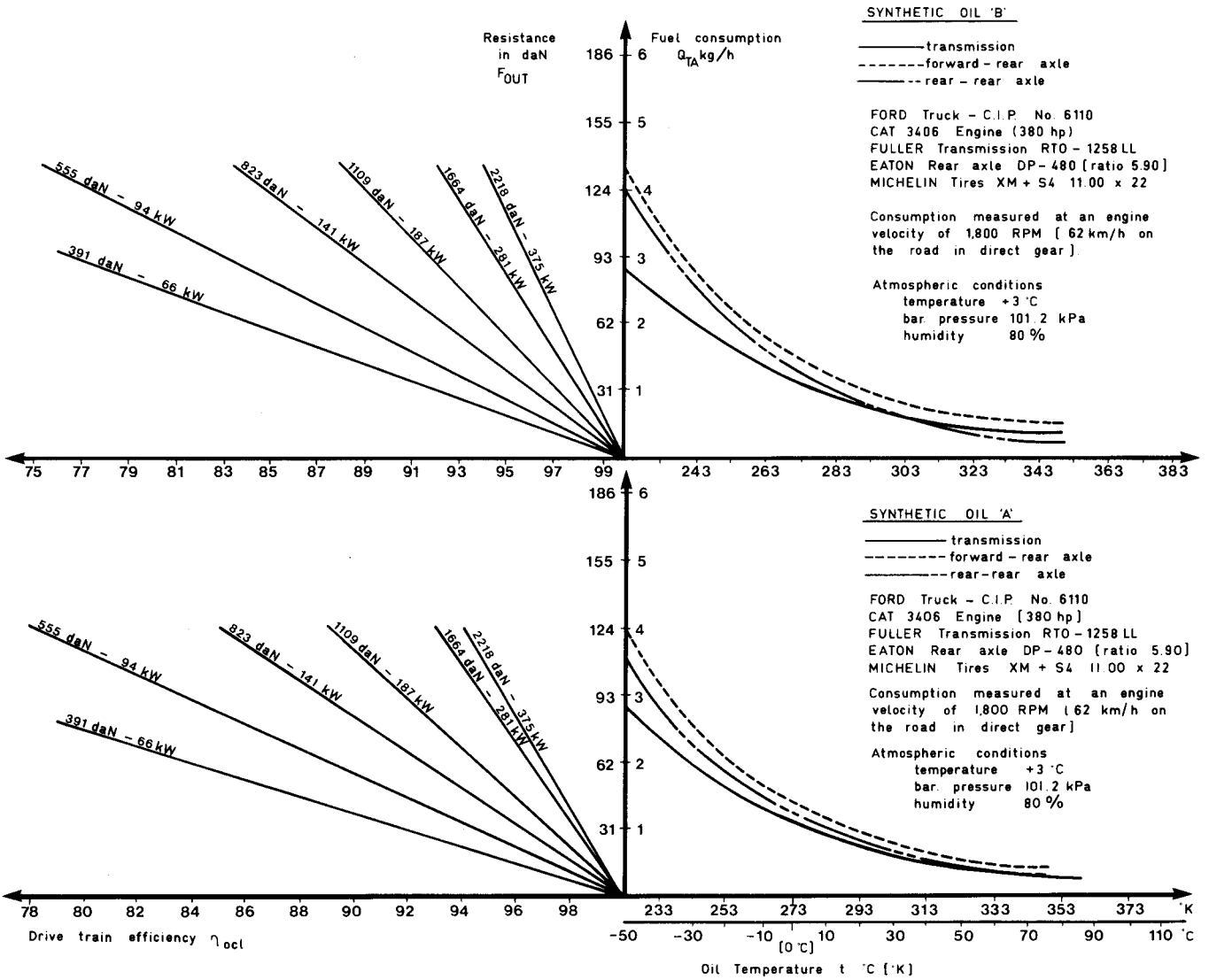


Figure 17 : Establishment of drive train efficiency coefficients in terms of oil temperatures for synthetic oils 'A' and 'B'.

Semi-synthetic and synthetic oils

Comparative tests were performed on the oils listed below in order to study the oil churning resistance effects of oils of different compositions.

- Standard
- Semi-synthetic "A"
- Semi-synthetic "B"
- Semi-synthetic "C"
- Synthetic "A"
- Synthetic "B"

Figure 18 gives the viscosity of some of these oils at semi-logarithmic scales for a temperature range of -40°C to 100°C . It shows differences in viscosity, particularly at normal operating temperatures, which obviously has a major impact on resistances and thus on fuel consumption.

Figure 17 gives (as in the case of standard oil) resistances (fuel consumptions) as a function of temperatures ranging from -50°C to $+80^{\circ}\text{C}$. The results are similar, although synthetic oil "A" shows slight superiority. This difference is also apparent on the viscosity curves.

These two diagrams (Figure 16 and 17) elicit a number of comments.

- 1) Resistances (fuel consumptions) related to oil churning for semi-synthetic and synthetic oils are considerably lower at low temperatures than those obtained with standard oil.

They are virtually identical above 70°C with standard oil showing a very slight superiority (see Figure 15) despite the synthetic oils featuring considerably lower viscosities than standard oil in this temperature range (see Figure 18). The fact that lower viscosity oils do not continue to reduce the resistances in the transmission and drive axles suggest that the lubricating film of synthetic oils may be less effective at these higher temperatures. This could permit an increase in the mechanical friction forces which more than cancel out any reduction in the oil churning resistance which might be expected from the reduced oil viscosities.

- 2) Let us compare the fuel consumptions derived from summing the resistances, of the transmission and drive axles with standard oil and synthetic oil "A". According to Figure 15 where fuel consumptions represent the totals for all three drive line components, for a total vehicle fuel consumption of 21 kg/h at mean road speed of 56 km/h, we obtain the following:

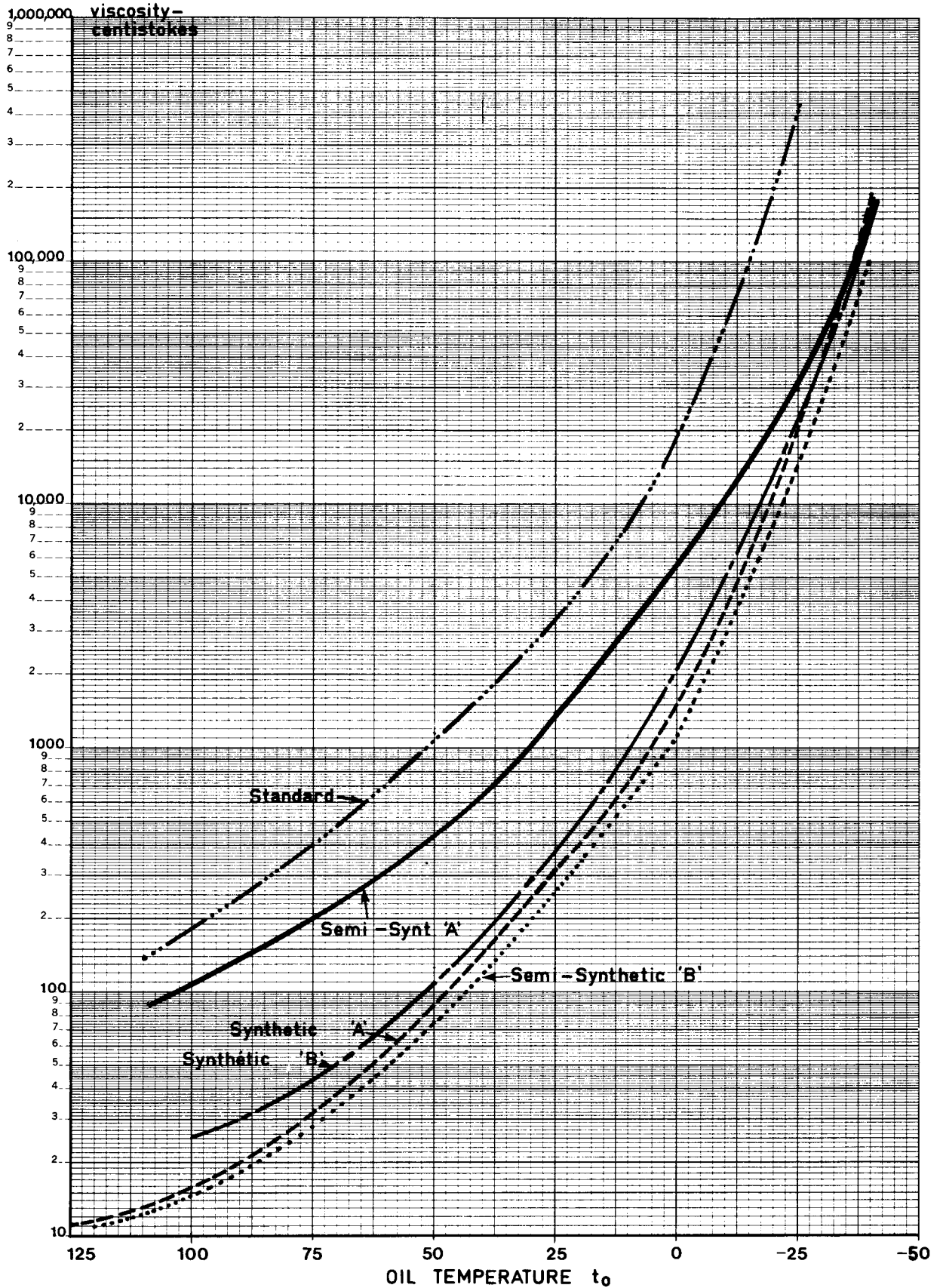


Figure 18 : Kinematic viscosity ASTM D-445 centistokes in terms of temperature (°C).

- (a) at 35°C (winter) operating oil temperature
- Consumption with standard oil: 2.76 kg/h
- Consumption with synthetic oil "A": 2.01 kg/h
 $\% \text{ difference in winter (35°C)} = \frac{2.76-2.01}{21} = 3.6\%$
 $\% \text{ difference in winter (35°C)} = \underline{3.6\%}$
- (b) at 60°C (summer) operating oil temperature
- Consumption with standard oil: 1.50 kg/h
- Consumption with synthetic oil "A": 1.30 kg/h
 $\% \text{ difference in summer (60°C)} = \frac{1.50-1.30}{21}$
 $\% \text{ difference in summer (60°C)} = \underline{1\%}$

The difference in fuel consumption during winter months is also indicated in Table 2 for consumptions calculated on the basis of the resistances for five oils. The results compare very favourably.

If the difference in fuel consumption between synthetic oil "A" and standard oil found on the road test with torque applied is compared for the oil churning loss only with the same temperatures (see Fig. 15 where the readings at 60°C are 1.50 and 1.30 kg/h respectively for standard and synthetic oils) the differences become:

- (a) With applied torque (see Table 3)
Difference = $\frac{7.19-6.93}{7.19} = 3.6\%$
- (b) Without applied torque (churning only)
Difference = $\frac{1.50-1.30}{7.19} = 2.8\%$

The difference in the lubrication properties of the two oils accounts for the 0.8% difference in fuel consumption.

- 3) The difference in fuel consumption with standard oil and synthetic oil "A" is about 3.6% with the Spicer transmission and Eaton DP-580 rear axle (Table 2) at the following oil temperatures:
- transmission 35°C
- forward-rear axle 30°C
- rear-rear axle 30°C

The difference for the Mack transmission and rear axle is 3.05% (Table 4). The 0.55 discrepancy between these two values is attributable to the transmission and rear axle design. The difference in Table 5 from another series of field tests is very similar, i.e. 0.4%.

TRUCK: PACIFIC P-512 (No. 2724) at Maclaren
 TRUCK: FORD No. 6110 at C.I.P. in Maniwaki
 ENGINE: CAT 3406, 380 (400) BHP
 TRANSMISSION: SPICER 1420-3A in the Pacific and
 FULLER RTO-1258 LL in the FORD
 AXLE: EATON DP-480 (580) P in all instances

SEASON	TEMPERATURE IN °C			OIL TYPE	FUEL CONS. IN kg/h	difference from Synt oil 'A' - %	TOTAL CONS. ②	OBSERVATIONS
	TRANSM.	F-R axle	R-R axle					
WINTER	35	30	30	Standard	2.76	+37	+3.6 %	average of 30 tests
	-II-	-II-	-II-	Semi-syn 'A'	2.03	+~1	negligible	average of 10 tests
	-II-	-II-	-II-	Semi-syn 'B'	2.25	+12	+1.1 %	average of 10 tests
	-II-	-II-	-II-	Synthetic 'A'	2.01	—	—	average of 30 tests
	-II-	-II-	-II-	Synthetic 'B'	2.16	+7.5	+0.7 %	average of 30 tests

- ① Consumptions calculated from the resistances and corrected to the same temperatures by extrapolation.
- ② Total fuel consumption difference from synthetic oil 'A'.

TABLE 2: Comparison of fuel consumptions (kg/h) through oil churning losses for different oils in the transmissions and rear axles. ①

barometric pressure	relative humidity	ambient temperature	engine oil temperature	engine coolant temperature	fuel temperature	transmission oil temperature	F-R axle temperature	R-R axle temperature	number of engine revolutions	road speed	total fuel consumption on road	difference as % of total fuel consumption	oil type
kPa	%	°C	°C	°C	°C	°C	°C	°C	RPM	km/h	kg/h	%	
100.6	57	+9	93	84	25	65	63	53	1586	12.5	7.19	+3.60 ①	Standard
101.5	48	+8	96	86	23.5	64	65	54	1584	12.5	6.93	—	Synthetic 'A'

① Average of 12 tests

Table 3: Comparison of fuel consumptions on the road (loaded vehicle) for standard oil and for pure synthetic oil 'A' in the transmission and drive axles (all other conditions being comparable).

- MACK Truck No. 6168 at Lake Ottawa (C.I.P.)

SEASON	TEMPERATURE IN °C			OIL TYPE	Fuel Consumption in kg/h	Difference in fuel consumption %	Difference in total fuel consumption % ②	OBSERVATIONS
	TRANS.	F-R AXLE	R-R AXLE					
WINTER	35	30	30	Standard	2.24	9	3.05	Average of 11 tests
	35	30	30	S. Synth. 'A'	1.60	—	—	Average of 9 tests

① Fuel consumptions calculated from the resistances and corrected for the same temperatures by extrapolations.

② Relative to total vehicle fuel consumption

TABLE 4: Comparison of fuel consumptions (kg/h) through oil churning losses in the transmissions and rear axles for standard and synthetic oils. ①

SEMI - SYNTHETIC OIL 'A' IN TRANSMISSION AND DRIVE AXLES

TESTS	TEMPERATURE IN °C			fuel consumption kg/h	DIFFERENCE in %	TRANSM	REAR AXLE	DIFFERENCE ②
	TRANSM.	F-R AXLE	R-R AXLE					
25.9.1982	35	30	30	2.03	+ 4.6	SPICER 1420-3A	EATON DP-580-P	+ 0.4
16.6.1982	35	30	30	2.37	+22.16	SPICER 1420-3A	ROCKWELL SU-170	+ 1.8
19.11.1982	35	30	30	1.94	+ —	Maxitorque TRLX 107	MACK	+ —

1 Consumptions calculated from the resistances and corrected for the same temperatures by interpolation

2 Difference in fuel consumption relative total.

TABLE 5: Comparison of fuel consumptions (kg h) through oil churning losses in the transmissions and rear axles. ①

F.1.1.2. Influence of transmission and rear axle designs

Table 5 gives the differences in fuel consumption or resistances for (a) Mack transmission and axles and (b) Spicer 1420-3A transmission coupled with an Eaton DP-580 or Rockwell SU-170 axle for the same transmission and rear axle oil temperatures. The figures show that the Rockwell axle-Spicer transmission combination absorbs the most power, while the Mack axle-Mack transmission setup absorbs the least power. The data in Table 5 point up the interest of pursuing investigation of variations in design and of confirming these findings through further testing. At that time the mechanical reliability and component life would have to be included before a valid economic analysis could be made.

G. INTERPRETATION OF RESULTS

G.O. DETERMINING COEFFICIENT η_{OCL} FOR OIL CHURNING LOSSES IN A POWER TRANSMISSION SYSTEM

Based on equation (6) given earlier, we have:

$$\eta_{DT} = \eta_{FR} (1 - F_{OC}/F_{OUT})$$

- where:
- η_{DT} overall drive train efficiency
 - η_{FR} efficiency coefficient of mechanical friction dependent on several factors. As we have yet to study this rating, we will calculate it by formula (7) and consider it set for our trucks at the empirical value calculated earlier, i.e. $\eta_{FR} = 0.92$. This value will be used from here on to calculate the overall drive train efficiency η_{DT}
 - F_{OC} force of resistance caused by oil churning, daN
 - F_{OUT} engine output power, daN

Then $(1 - F_{OC}/F_{OUT})$ defines the coefficient for oil churning losses in a power transmission system or $(1 - F_{OC}/F_{OUT}) = \eta_{OCL}$.

To obtain efficiency η_{OCL} under the conditions given in Figure 14 for standard oil, we plot the oil temperature for each component on the X-axis of Figure 16, then draw a vertical line to the point of intersection with its curve and read the corresponding resistance (consumption) on the Y-axis. We add up the resistances of the three components and plot the result on the Y-axis. We draw a horizontal line to the left up to the straight line representing engine output power F_{OUT} in daN and return to the X-axis to read efficiency η_{OCL} . Lastly, using formula (6), we calculate overall efficiency η_{DT} by multiplying coefficient η_{FR} by coefficient η_{OCL} .

G.1. SAMPLE APPLICATIONS UNDER ACTUAL OPERATING CONDITIONS

- (a) It is now possible to determine coefficient η_{OCL} using the following example.

Temperatures were measured for the situation described in Table 5:

- . transmission 35°C
- . forward-rear axle 30°C
- . rear-rear axle 30°C

Figure 16 gives ~21 daN for the transmission, ~35 daN for the forward-rear axle and ~24 daN for the rear-rear axle. These resistances total 80 daN.

We will also calculate mean engine output power corrected for the wheels for a situation in which road consumption is 21 kg/h (6 mpg for a mean road speed of 56 km/h). As the mean engine rotating velocity at 56 km/h is roughly 1,800 RPM in direct gear, we have (load and no-load):

$$F_{OUT} = 684 \text{ daN (106 kW)}$$

and

$$\eta_{OCL} = 1 - \frac{80}{684} \qquad \eta_{OCL} = 0.88$$

Thus, 12% of the engine output power is expended to churn the oils under normal operating conditions.

Going on to multiply η_{OCL} by efficiency η_{FR} , we obtain overall drive train efficiency η_{DT} to be:

$$\eta_{DT} = 0.92 \cdot 0.88 = 0.81$$

- (b) Let us now consider the same situation but with the oil temperatures as given below:

(never experienced during field tests, even with ambient temperatures up to $+40^{\circ}\text{C}$).

- . transmission 80°C
- . forward-rear axle 80°C
- . rear-rear axle 80°C

These resistances total ~ 31 daN.

Engine output power (corrected for the wheels) for the same conditions will be $F_{\text{OUT}} = 684 - 50 = 634$ daN. Thus, the coefficient for oil churning losses

$$\eta_{\text{OCL}} = 1 - \frac{31}{634} = 0.95$$

and the drive line efficiency

$$\eta_{\text{DT}} = 0.95 \cdot 0.92 = 0.88$$

In this case we come close to the efficiency of $\eta_{\text{DT}} = 0.85$ commonly given in the technical manuals.

This difference between measured and published drive train efficiency does not take into account the oil heating time from start-up until stabilized temperatures have been reached. During this period even lower temperatures and thus higher resistances are experienced. For the conditions experienced in Canadian logging operations the drive line efficiency published in technical manuals would appear to be too high and should be adjusted for the actual oil temperatures experienced.

G.2. COMPARISON OF RESULTS FOR STANDARD OIL AND SYNTHETIC OIL UNDER ACTUAL OPERATING CONDITIONS

Comparison at 35°C

Force required to churn the oil in the power transmission system, F_{OC}

- Standard oil $F_{\text{OC}} = \sim 80$ daN
- Synthetic oil "A" $F_{\text{OC}} = 63$ daN (from Figure 17)

Engine output power, F_{OUT}

- Standard oil $F_{\text{OUT}} = 684$ daN
- Synthetic oil "A" $F_{\text{OUT}} = 634$ daN

Thus, coefficient of drive train losses:

- Standard oil $\eta_{DT} = (1 - \frac{80}{684}) = 0.88$

- Synthetic oil $\eta_{DT} = (1 - \frac{53}{634}) = 0.92$

Difference in drive train losses between the two oils at 35°C:

Difference (35°C) = 4%

The difference at 80°C is minimal provided that the other properties of synthetic oils are disregarded.

The preceding findings show that a fuel consumption gain can be achieved in one of two ways: by using synthetic oils or devising some means of heating the oils. Naturally, the second alternative is more interesting, although we should bear in mind there may be an advantage from some synthetic oils for friction reduction owing to certain antifric-tion properties, but provided there are no adverse related maintenance or component life factors.

G.3. STARTING AND OPERATING WITH COLD OILS

Figures 19-21 are diagrams that relate the temperature of a given oil in the transmission and rear axle to resistance F_{OC} through oil churning or to fuel consumption on the one hand and to oil viscosity on the other.

At low temperatures the resistances related to oil churning are clearly very high because of high oil viscosity. Consequently, cold starting not only becomes very difficult but adds to excessive wear of the engine and drive train.

It would therefore be desirable to preheat the transmission and rear axle oils, as is done for the engine oil and coolant. The oils could be electrically preheated while the trucks are at a standstill between shifts.

We see from Figure 22 that at an ambient temperature of -20°C, it takes roughly three hours in operation to reach stable maximum temperatures. If the oils are not heated, power consumption during that time is even greater than indicated by the above comparison (Section G.2). Under summer conditions with the ambient temperature +15°C, the time required for the oils to reach maximum stable temperature is still about 90 minutes. (Figure 23).

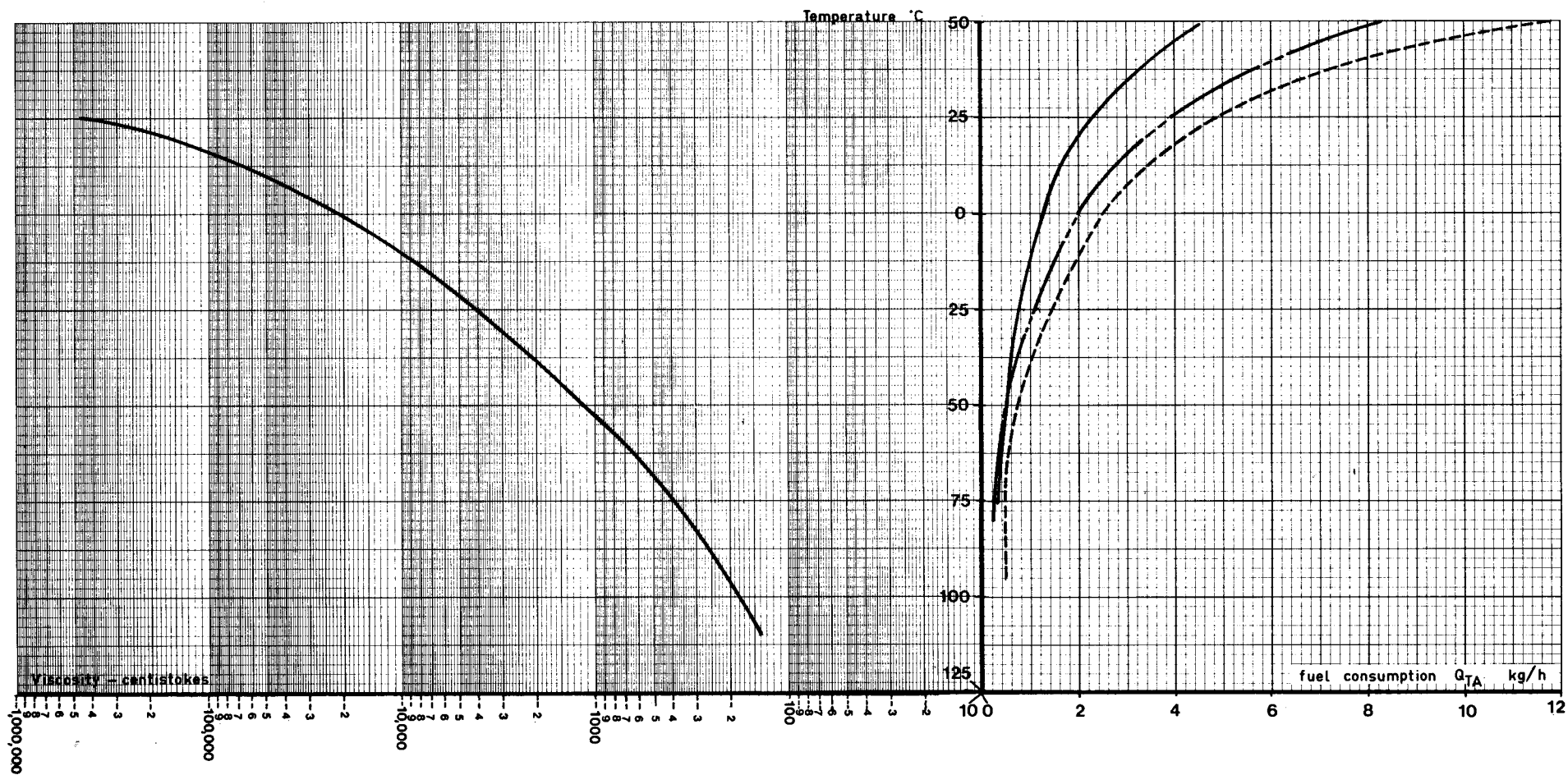


Figure 19 : Relationship between viscosity, oil temperature and fuel consumptions [from oil churning only] for standard oil.

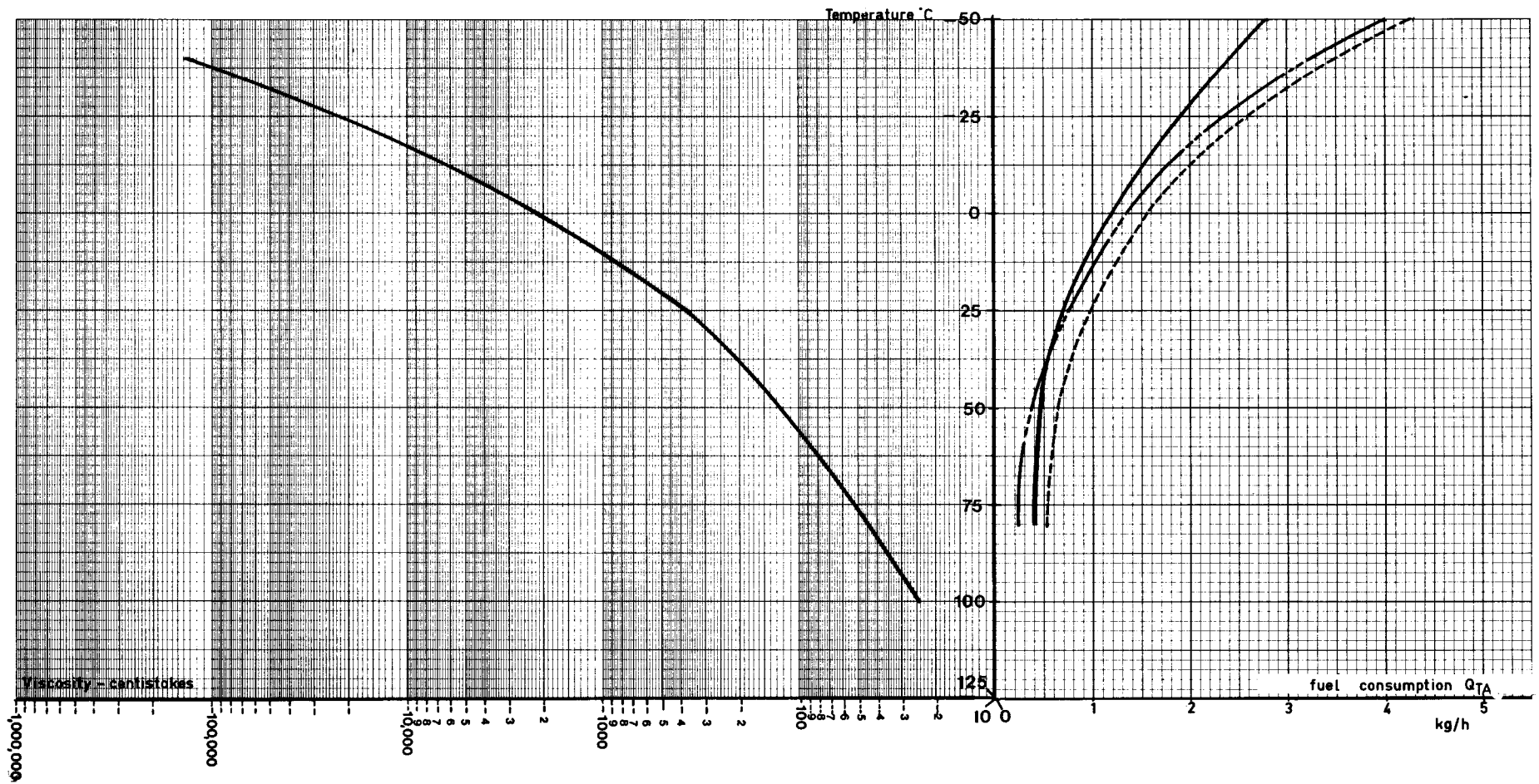


Figure 20 : Relationship between viscosity oil temperature and fuel consumptions (from oil churning only) for synthetic oil 'B'.

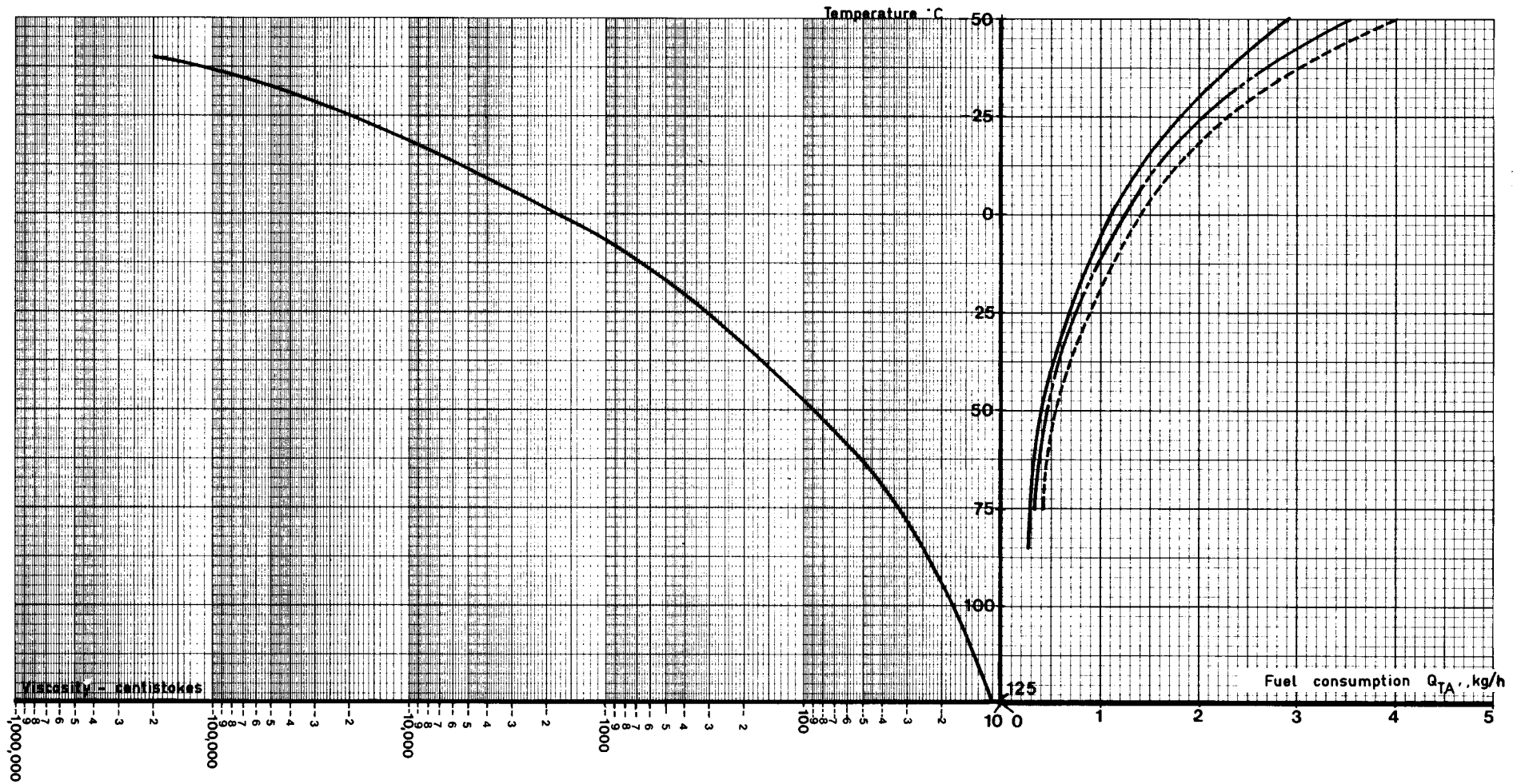


Figure 21 : Relationship between viscosity, oil temperature and fuel consumptions (from oil churning only) for synthetic oil 'A'.

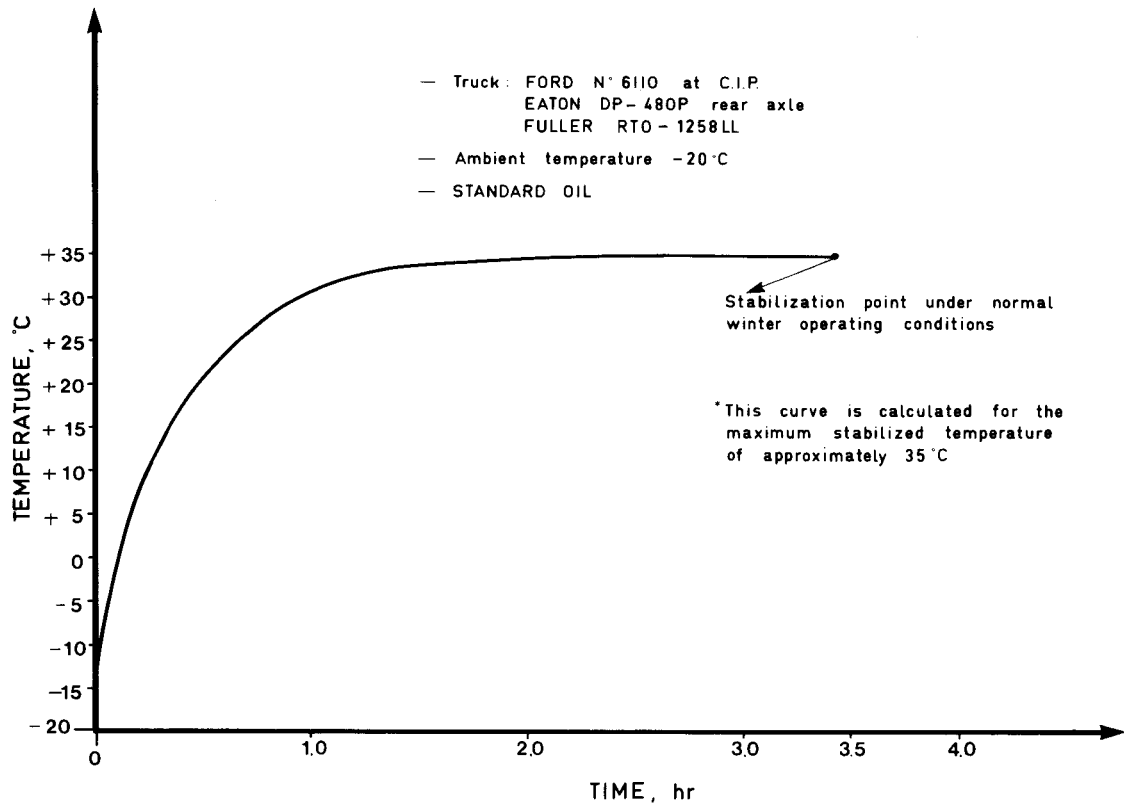


Figure 22 : Build-up of transmission and rear axle oil temperatures during winter operation.

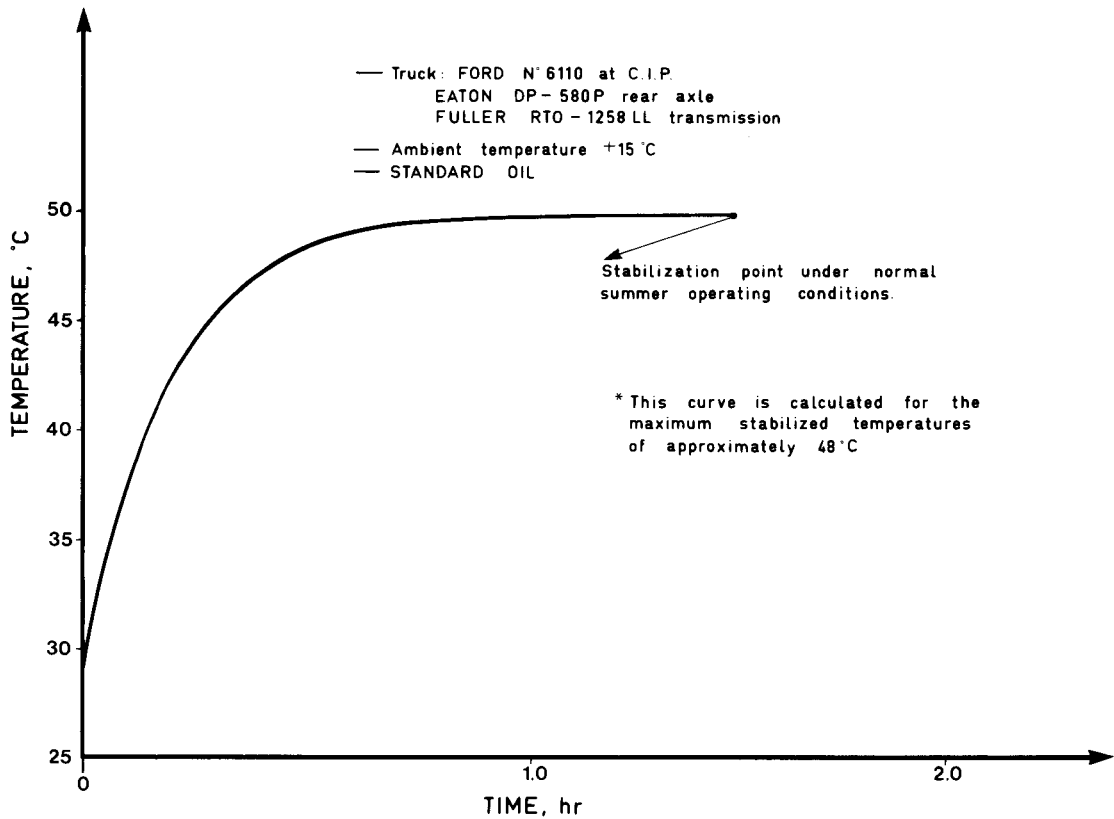


Figure 23: Build-up of transmission and rear axle oil temperatures during summer operation.

H. SAMPLE CALCULATION OF POTENTIAL FUEL SAVINGS IN TERMS OF OPERATING CONDITIONS

In Figures 22 and 23 the temperature-time relationship is plotted for the time (hours) from start-up to stabilization of transmission, forward-rear axle and rear-rear axle oil temperatures at a maximum temperature, for a given ambient temperature and actual operating conditions.

Based on Canadian Meteorological Service data on daily temperatures for Northern Québec, we calculated the mean day and night temperatures in winter (-20°C) and in summer ($+15^{\circ}\text{C}$). Upon calculating the build-up of oil temperatures in terms of operating time, we used these two mean ambient temperatures.

In the two following examples of simulated hauling operations it has been assumed that the resistance of standard oil to churning can be obtained by lowering its viscosity through raising its temperature to a controlled $+80^{\circ}\text{C}$. The alternative is to use synthetic or semi-synthetic oils which have lower viscosities than standard oil at similar temperatures. This was the option used in the example of actual operations results which has been given.

H.O. CALCULATING POTENTIAL FUEL SAVINGS DURING WINTER MONTHS (-20°C MEAN AMBIENT TEMPERATURE)

To calculate in-service savings, we used this scenario for a normal hauling operation:

- 1) The truck starts out in the morning with the oils at about -5°C (the oils have not had time to cool completely since the previous shift).
- 2) It takes 0.75 hour to load the truck. During this time, the truck is at a standstill and the oil temperature does not rise.
- 3) The loaded truck starts out on the road and travels 100 km (60 miles) at a mean speed of 56 km/h. Thus, $100/56 = 1.8$ hours. The oil temperature (see Figure 22) rises -5°C to about $+33^{\circ}\text{C}$, averaging $(33+5)/2 = 19^{\circ}\text{C}$.
- 4) The truck stops for 0.5 hour for unloading, during which time the oil temperature drops roughly 15°C , i.e. to $+18^{\circ}\text{C}$.
- 5) The truck restarts at no-load and returns along the same route. The oil temperature rises from 18°C during this run (50 minutes) but not as rapidly as with the truck loaded and reaches about 30°C . The average temperature this time is $+24^{\circ}\text{C}$.
- 6) While the truck is being reloaded (0.75 hour), the driver takes his lunch break and the oil temperature drops again by 20°C , to $+10^{\circ}\text{C}$.
- 7) The truck restarts and makes the run in 1.8 hours. The oil temperature rises from 10°C to $+32^{\circ}\text{C}$. Average 21°C .

- 8) The truck is unloaded in 0.5 hour, during which time the oil temperature drops 10°C , to $+22^{\circ}\text{C}$.
- 9) The truck returns at no-load in 0.83 hour and the oil temperature rises 10°C , to $+32^{\circ}\text{C}$. Average 21°C .
- 10) The truck reloads (0.75 hour) and the oil temperature again drops to 20°C .
- 11) The loaded truck makes the run in 1.8 hours and the oil temperature rises from 20°C to $+35^{\circ}\text{C}$. Average 27.5°C .

In this scenario the shift is completed in roughly 10 hours.

Total operating time on the road is 5.26 hours:

- with load: 3.60 hours at a mean temperature of 23.3°C .

- no load: 1.66 hours at a mean temperature of 22.5°C .

The overall average is 23°C .

If we now refer back to Figure 15 for the fuel consumption at a mean temperature of 23°C , we read (for hourly consumption of some 21 kg/h):

- 1) at 23°C $Q_{\text{TA}} = 3.3 \text{ kg/h}$
- 2) at 80°C $Q_{\text{TA}} = 1.0 \text{ kg/h}$

The potential total fuel savings in winter if the transmission and axle oil temperatures can be maintained at 80°C becomes:

$$\frac{3.3}{21} - \frac{1}{21} = \sim 11.0\%$$

H.1. CALCULATING POTENTIAL FUEL SAVING DURING SUMMER MONTHS (+15 $^{\circ}\text{C}$ MEAN AMBIENT TEMPERATURE)

We will consider here the same shift duty cycle as described for winter-time operations. Then the oil temperatures become:

- 1) Starting temperature $+25^{\circ}\text{C}$
- 2) No change
- 3) Run in 2.30 hours. Final temperature $+55^{\circ}\text{C}$. Average $+40^{\circ}\text{C}$
- 4) The temperature drops 10°C , to $+45^{\circ}\text{C}$
- 5) The temperature rises to $+55^{\circ}\text{C}$. Average $+50^{\circ}\text{C}$
- 6) The temperature drops 15°C , to $+35^{\circ}\text{C}$
- 7) The temperature rises 20°C , to $+55^{\circ}\text{C}$. Average $+45^{\circ}\text{C}$
- 8) The temperature drops to $+35^{\circ}\text{C}$
- 9) The temperature rises to $+55^{\circ}\text{C}$. Average $+45^{\circ}\text{C}$
- 10) The temperature drops to $+45^{\circ}\text{C}$
- 11) The temperature rises to $+55^{\circ}\text{C}$. Average $+50^{\circ}\text{C}$

The overall average for the shift is 46°C . Reading now the fuel consumptions required to overcome the oil churning resistances at 46°C and 80°C on Figure 15, we observe:

- 1) at $+46^{\circ}\text{C}$ $Q_{\text{TA}} = 1.60 \text{ kg/h}$
- 2) at $+80^{\circ}\text{C}$ $Q_{\text{TA}} = 1.00 \text{ kg/h}$

The potential savings in summer if transmission and axle oil temperatures can be maintained at +80°C would be:

$$\frac{1.60}{21} - \frac{1.00}{21} = 3.0\%$$

Fuel gain in summer: 3.0%

The average fuel savings over the entire year by heating the oils to +80°C is roughly 8%.

Field results comparing standard and semi-synthetic oils

To confirm these results under actual operating conditions, we monitored the fuel consumption of two trucks at Maclaren. Following are our results:

1) Pacific truck model 2757 operating on semi-synthetic oil

- September consumption	6,504 litres in 311.5 hours
- October consumption	<u>7,983 litres in 377 hours</u>
total	14,487 litres in 688.5 hours

This gives 21.04 L/h

2) Pacific truck model 2756 operating on standard oil

- September consumption	6,080 litres in 253 hours
- October consumption	<u>7,605 litres in 306 hours</u>
total	13,685 litres in 559 hours

This gives 24.48 L/h

Difference ≈14%

Naturally we are dealing here with two trucks having similar specifications and operating under the same conditions though with different drivers. Slight differences in fuel consumption are thus possible. Nevertheless, this provides rather convincing confirmation of the value derived by the previous calculations.

The temperatures used in this report are usually those recorded during our tests. Only a few were taken from trucks (loaded or empty) in actual service. To confirm our observations, we therefore measured temperatures directly from loaded vehicles during operations. Based on those temperatures, we calculated the stabilization temperatures, which range around 35°C during the winter. In order to complete this study, temperatures would have to be continuously recorded on vehicles in service during both winter and summer. Only then will we have a complete picture of the conditions under which the transmissions and axles operate.

To complete the study of power losses from drive line resistances, it will be necessary to measure and analyse the losses through mechanical friction upon application of torque. This is scheduled to be carried out in early 1984 in the FERIC transport research program.

I. CONCLUSION

This second report in the series titled Analysis of productivity and cost of forestry transportation focuses on analysis of the forces of resistance from oil churning in the transmission and rear axles. It also presents a theoretical analysis of the energy balance, which will provide the basis for future research on the duty cycle of road vehicles.

The results written up in this report show that the industry would do well to test the use of certain high-grade synthetic oils and, even more, search for a practical system for heating the transmission and drive axle oils.

It would further be in the industry's interest to mount thermometers on the transmissions and rear axles of its trucks--insofar as this is feasible--in order to keep track of the temperatures and gain a clearer picture of the conditions under which lubrication takes place.

The report contains two diagrams (Figures 16 and 17) that can aid in determining oil churning losses for the appropriate oils using the temperatures which would be thus obtained. For practical purposes these diagrams indicate the drive train oil churning losses for all commonly used types and makes of transmissions and rear-axles and the savings which can be realized by modifying the oil viscosities through oil selection or by increasing oil temperatures.

The appendix contains a description of the instrumentation and testing methods used.

J. APPENDIX

J.O. DETERMINING THE MOMENT OF INERTIA J_{WT} OF A TIRE WITH WHEEL
(daN·m·sec²)

To determine the moment of inertia of a wheel rotating on its axis on a decline, we use the diagram below (Figure 24).

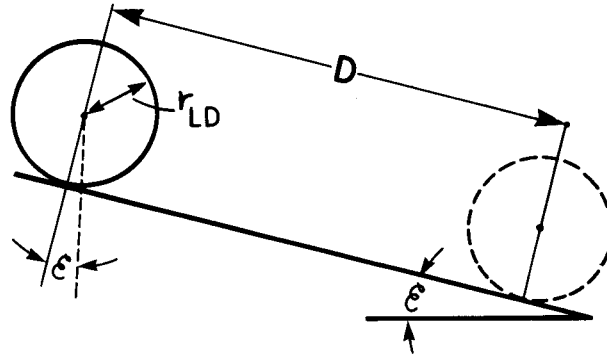


Figure 24 : Diagram of a wheel rolling on a decline.

- where:
- G_W mass of wheel with tire, kg ($G_W = 109.31$ kg)
 - D distance, m
 - t_D time taken to travel distance D
 - r free radius of tire, m
 - J_{WT} moment of inertia, daN·m·sec²

Force of acceleration $F_a = G \cdot \sin \epsilon$

The force of inertia to be overcome is:

$$F_a = M \cdot a_a = \frac{G_W}{g} \cdot a_a \quad (51)$$

This force is equal to:

$$F_a = \frac{2G \cdot D}{g \cdot t_D^2} \quad \text{since } D = \frac{1}{2} a_a \cdot t_D^2 \quad (52)$$

The relative inertia to be overcome is equal to (see formula (20) in report TR-53):

$$F = J_{WT} \cdot \frac{a}{r_{FR}^2} \quad (53)$$

thus:

$$F = G_W \sin \epsilon = \frac{2 \cdot G_W \cdot D}{g \cdot t_D} + \frac{2 \cdot J_{WT} \cdot D}{r_{FR}^2 \cdot t_D} \quad (54)$$

from which:

$$G_W \cdot \sin \epsilon = \frac{2 \cdot G_W \cdot D}{g \cdot t_D} \left[1 + \frac{J_{WT} \cdot g}{r_{FR}^2 \cdot G_W} \right] \quad (55)$$

and:

$$J_{WT} = \frac{r_{FR}^2 \cdot G_W}{g} \left[\frac{g \cdot t_D^2 \cdot \sin \epsilon}{2D} - 1 \right] \quad (56)$$

Using this equation, we will establish J_{WT} for the wheel and the tire corresponding to the wheels mounted on the test trucks (Michelin 11.00 x 22, type x M + S4).

Test results:

- G_W 109.31 kg
- D 34.98 m
- d wheel diameter 1.1135 m ($r_{FR} = 0.55675$ m)
- t_D 14.36 D
- $\sin \epsilon = 0.055811$

Introducing these data in equation (56) gives:

$$J_{WT} = \frac{0.55675^2 \cdot 109.31}{9.8182} \left[\frac{9.8182 \cdot 14.36^2 \cdot 0.0558}{2 \cdot 34.98} - 1 \right]$$

$$J_{WT} = 2.12 \text{ daN} \cdot \text{m} \cdot \text{sec}^2$$

The moment of inertia of the same wheel calculated by formula (18) in report TR-53 is equal to:

$$J_{WT} = \frac{0.0245 \cdot 3016.5 \cdot 0.283}{9.8182}$$

$$J_{WT} = 2.13 \text{ daN} \cdot \text{m} \cdot \text{sec}^2$$

J.1. TESTING METHODS

In its series of studies on forestry transportation, FERIC not only employs the standard laboratory tests but also uses vehicles in actual operation in their normal work environment and in different atmospheric conditions. This required the cooperation of forestry enterprises which made production units available for these tests. FERIC was also obliged to design new measuring devices or modify existing ones (theoretically designed for laboratory use) and adapt them for moving vehicles so that they resist vibration, acceleration, shock and inclement weather. These instruments must still yield results as close as possible to those obtained in a stationary laboratory. While we were pursuing results, we also had to gain experience in the use of the testing methods and instrumentation and in coordinating operations.

The results written up in this report and those to come are based on the analytical methodology described in report TR-53. Let us briefly review the coast down method.

Coast down testing with the drive wheels elevated

The deceleration of the wheels and power transmission system is logged while recording the original, intermediate and zero speeds as well as the time between these three speeds. These data are sufficient to determine the initial force of resistance F_{OC}° owing to oil churning at low speed and coefficient a^* , representing the rate of increase of losses in the power transmission system as determined by the increase in speed.

These data are obtained by means of a special device proposed by FERIC and actually built by Ruhl Machinery. They can also be recorded with an instrument devised by FERIC (see Figures 30 and 31).

* This coefficient has been defined in TR-53 report.

Coast down test with a loaded truck-trailer on the road

The deceleration is measured on a flat, straight strip of road in both directions (to minimize the effect of wind and slope), first from high to lower speed and then from low to zero speed. These tests are run twice, once at normal load and again at reduced load.

Deceleration from low to zero speed provides the data to calculate the initial force of resistance on the road, comprising the oil churning resistance (F_{OC}°)* and road rolling resistance $P_{f\Sigma}^{\circ}$. ($P_{tp}^{\circ} + P_{f\Sigma}^{\circ} = P_{fa}^{\circ}$ in report TR-53).

Decelerating from high to lower speed provides the data to calculate the coefficient for the rate of increase of the tire rolling and air resistances as determined by the increase in speed (c in report TR-53). To separate these two resistances, which are combined in coefficient c, we perform two deceleration runs with two different loads. This enables the calculation of the rolling resistance coefficient (k in report TR-53) and the air resistance coefficient (K in report TR-53). The means of calculating this separation is described in the aforesaid report.

The instrumentation is the same as used for testing with the drive wheels elevated.

All of these tests are accompanied by fuel consumption measurements (see instruments in Figures 27-29).

J.2. INSTRUMENTATION

When FERIC first started its transportation study it became increasingly clear that equipment designed for this purpose was not readily available. The problem encountered was that most of the scientific equipment which could have been used was either too bulky or too fragile to be mounted on a moving truck. Much time was spent experimenting with the available equipment and the optimal specifications were arrived at. The majority of instruments subsequently chosen were not originally meant for automotive use and were modified to suit the purpose. The lack of certain devices prompted FERIC to develop and build these, or contract out the work when machining facilities were needed. The instruments used at present are relatively inexpensive, robust, accurate and are adequately reliable.

* P_{tp}° in the TR-53 report

Temperature Measurement and Control:

Thermocouples: These are immersed in the medium, the temperature of which must be measured. The low mass of thermocouples permits them to react quickly to changes in temperature, and their simplicity makes them inexpensive. The working principle of these devices makes them compatible with a number of other instruments. Models used in the study have stainless steel casings, ceramic filler, and use "J" type copper-constantan connections.

Electronic Thermometer: Used in conjunction with the thermocouple and a properly insulated thermocouple wire, its micro-processor permits the user to obtain accurate measurements as far as thirty five meters from the source. Graduations are in tenths of degrees and are shown in the Fahrenheit or Celsius scales on a liquid crystal display. The model employed is intended for medical use and its diminutive size makes it suitably portable.

Source Selector: As the thermometer is designed to operate with a single thermocouple, a six channel thermocouple selector enables the operator to measure six temperatures from the same location. The thermocouple wires are connected to this device as well as is the thermometer. The selector itself is an integral part of the Ruhl (FERIC) datamaster described later on.

Thermo-Controllers: When temperature control is needed, the thermo-controller, using a thermocouple as reference, actuates a circuit breaker which can activate or deactivate a heat generating device. Threshold temperatures, ranging from 0^oF to 999^oF, are set manually on a digital scale.

Revolutions Transducer:

Pulse Sending Units: These compact devices, mounted on the tachometer cable bracket and on the speedometer gear assembly, convert revolutions to electrical pulses. These are generated by means of a miniature magneto in the device and travel through a three wire cable to the desired instrument. The pulse sending unit was designed specifically for automobiles and is consequently waterproof and shockproof (see Fig. 25).

Fuelmeters:

Batch Volumetric: This instrument, devised by FERIC, comprises a 250 ml graduated burette, two solenoid three way valves, and a diaphragm transfer pump. It is mounted in line to the existing fuel lines which means the vehicle can operate unhindered when the instrument is not in use (true for all fuel meters described later on). To operate this fuel meter

one must first fill it using the injectors return. This is done by throwing a switch which in turn activates the solenoid valve which diverts fuel flow going to the truck's fuel tank to the burette. Once the burette is filled testing can take place. During testing the burette acts as a miniature fuel reservoir; fuel is removed by diverting the coming flow from the fuel tank to the burette, and fuel is returned to the burette from the engine as described before. When testing is complete the valves are deactivated and flow returns to normal (see Fig. 26).

Batch Weight: In this case, fuel mass serves as the measuring variable. A preweighed interchangeable sample bottle, fitted with an insert containing two pipes, serves as the source of fuel during testing. The pipes, one for fuel return, the other for fuel feed, are each joined to solenoid three-way valves. These valves divert fuel flow to the bottle, from the truck's reservoir. The bottles are reweighed following completion of the tests. The difference in weight is the fuel consumption, within a twentieth of a gram. This system was designed by FERIC (see Fig. 27).

Continuous Volumetric: This apparatus was bought ready-made. It hooks into the existing fuel lines and can be bypassed if breakage occurs. The fuel return line and reservoir suction lines are connected to a deaeration chamber. This chamber also serves as a flow regulator by means of a float operated valve (similar to that found in plumbing). As the deaeration chamber empties, the float descends, opening the valve, thus allowing fuel to flow in through the fuel supply line. The fuel in the supply line comes from the fuel tank by the vehicles transfer pump and by a diaphragm pump in the fuelmeter. The fuel then goes through a fine filter and a turbine type volumetric transducer. The pulses and voltages from the latter are translated into liters and centiliters on a display in the cab. After passing through the turbine, the fuel flows to the deaeration chamber via the float valve and mixes with the return fuel before going to the injector pump (see Fig. 28).

Metering Instruments:

Initial Instrument Group: This comprised of an electronic Kienzle tachograph, a revolution accumulator and liter counter. The instrument was specified by FERIC and its construction contracted out by Ruhl Machinery. It was later modified to register two speed scales and rearranged to minimize its size. Electrical pulses generated by sending units and the continuous volumetric fuel meter are converted into instantaneous readings on its displays (see Fig. 29).

Ruhl (FERIC) Datamaster: Unlike the initial instrument group, which comprises the tachograph and liter counter, this device does not include any mechanically operated displays, thus making it less susceptible to error caused by vibration. Displays are either light emitting diode or liquid crystal. All information provided by the sending units and fuelmeter is processed electronically enabling it to produce the following data: three speeds (original, intermediate, and final speeds obtained in tests), two distances (distance covered in two time increments) accumulated revolutions, instantaneous revolutions and fuel accumulated consumption. Additionally the datamaster includes two chronometers and serves as control unit to a multichannel recorder (see Fig. 30 and 31).

Information Recording Instrument:

FERIC Data Logger: A multichannel recorder and microprocessor are at the heart of this instrument. Pulse information from sending units are translated to revolutions and distance by the microcomputer, stored in a memory, and later recorded on a cassette. The datalogger was specified by FERIC and conveyed by a local university. Concurrently, a second instrument was also developed which transfers data stored on cassettes, to FERIC's computer.

Peripheral Equipment:

Heat Exchange System: When performing tests which require temperature control of oils or fuel during winter months, use of this system is required. Hot engine coolant is circulated through three heat exchangers (two for fuel and one for transmission oil) and a water jacket fitted on the axle differential covers. Water circulation is achieved through use of an electric pump and temperatures are controlled with valves activated by the thermo-controllers (described previously). Additionally, an electrically heated hose further heats fuel going to the engine, and filters can be warmed overnight with plug-in-type battery warmers (see Fig. 32 and 33).

Transmission Oil Pump: Normally used with a cooling element, it is used in this case to transfer oil to the heat exchanger described above. The pump comes as a kit and is bolted to the transmission countershaft.

Voltage Inverter: Some of the equipment described earlier, such as the solenoid valves used to control temperature, and thermocontrollers, were not compatible with automotive electrical systems. In such cases the voltage inverter serves to convert twelve volts direct current, to a square wave one hundred and twenty volts alternative current.

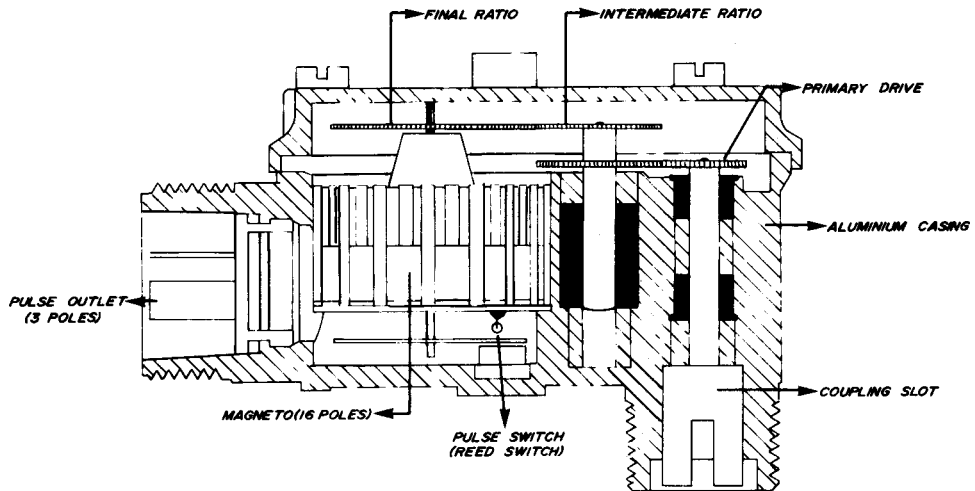


Figure 25: Cross-section of pulse sending unit used for speed measurements.

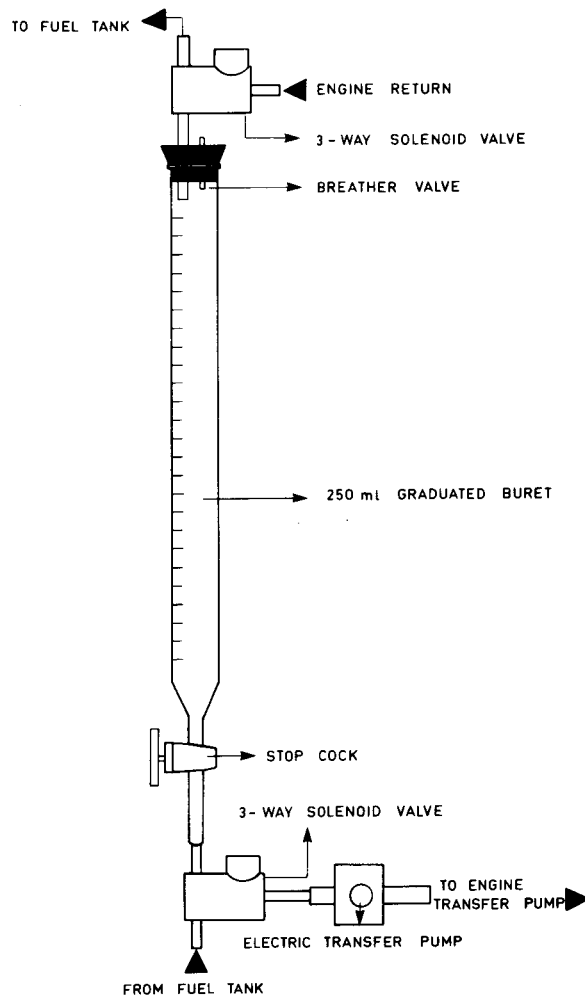


Figure 26: Diagram of batch volumetric fuelmeter (FERIC).

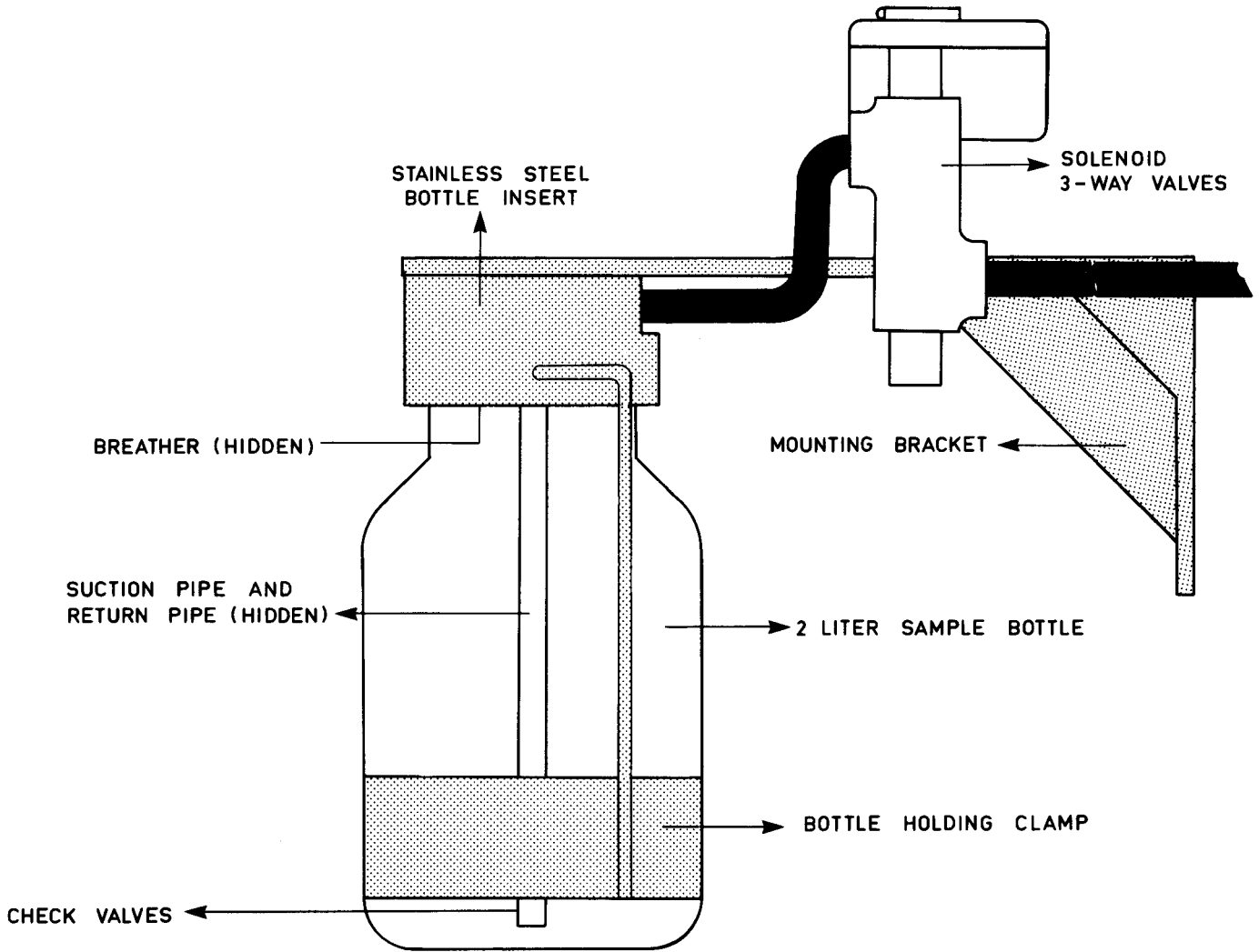


Figure 27: Diagram of batch weight fuelmeter (FERIC).

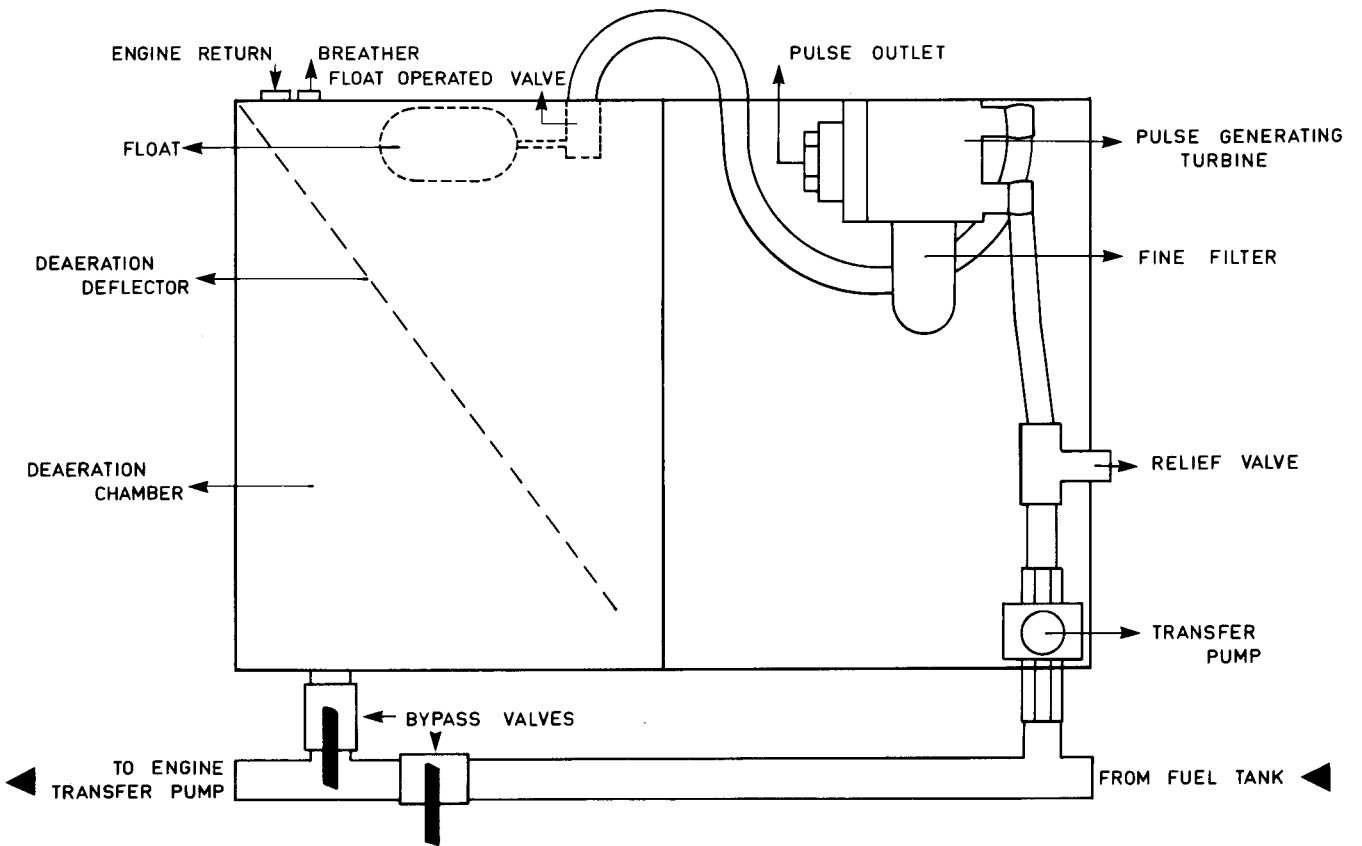


Figure 28 : Diagram of continuous volumetric fuelmeter (RUHL).

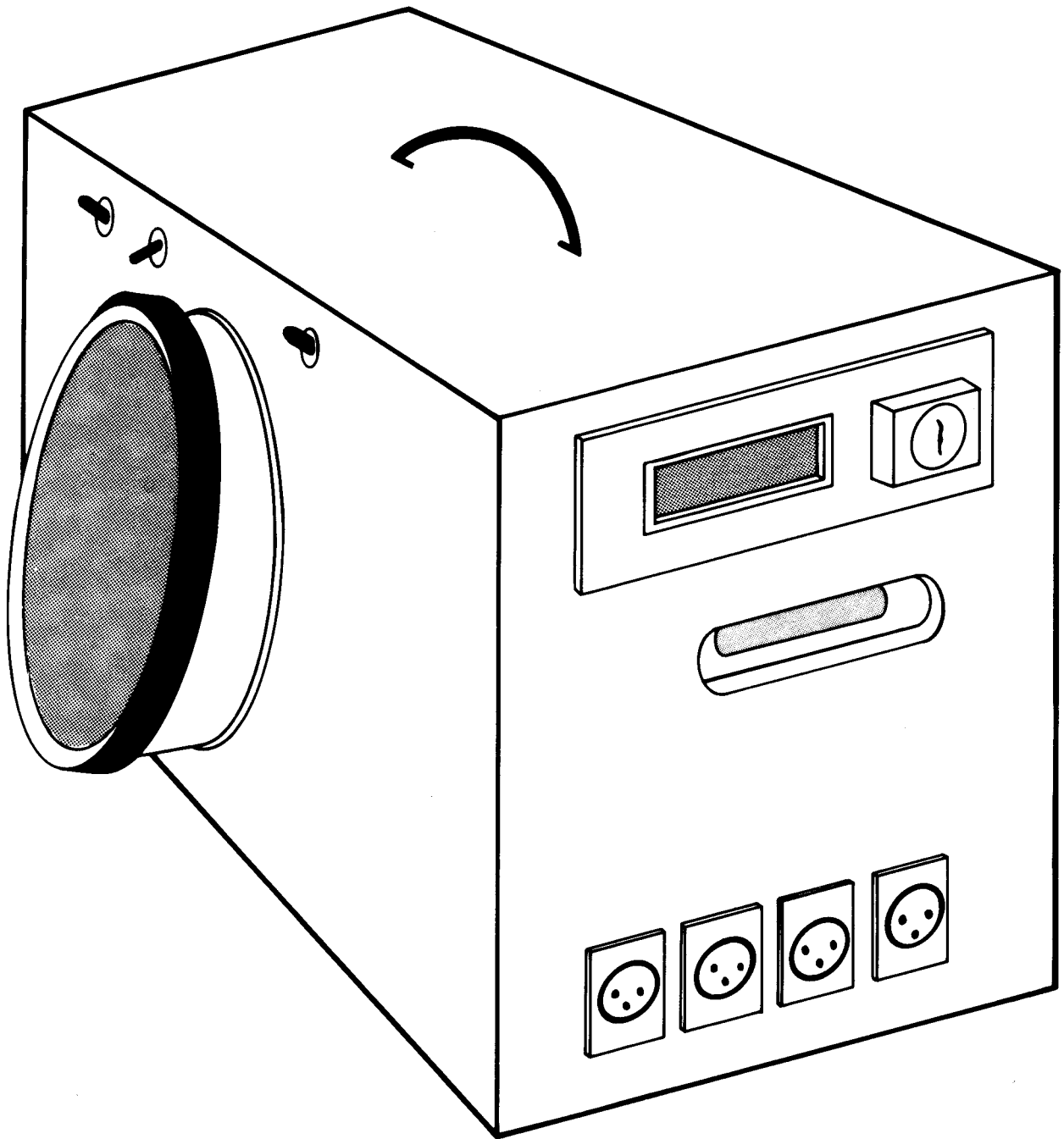


Figure 29 : FERIC Initial Instrument Group. Top right: electronic tachograph. Top left: revolution accumulator. Center: liter counter. Bottom: wire connectors.

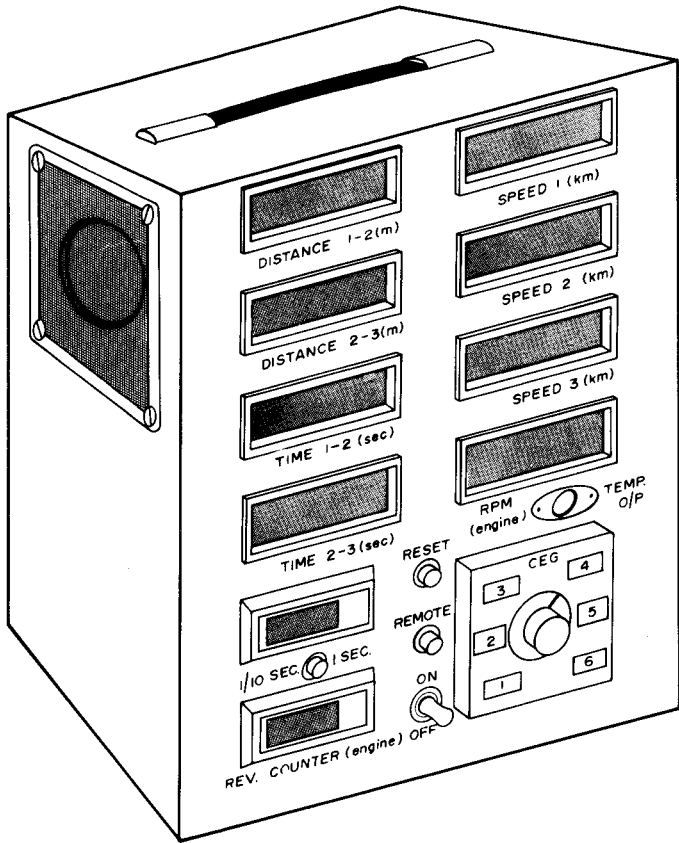


Figure 30: FERIC DATAMASTER. Front view: The displays are either LED or LCD. A 6-channel thermocouple selector is located to the right of the on/off switch.

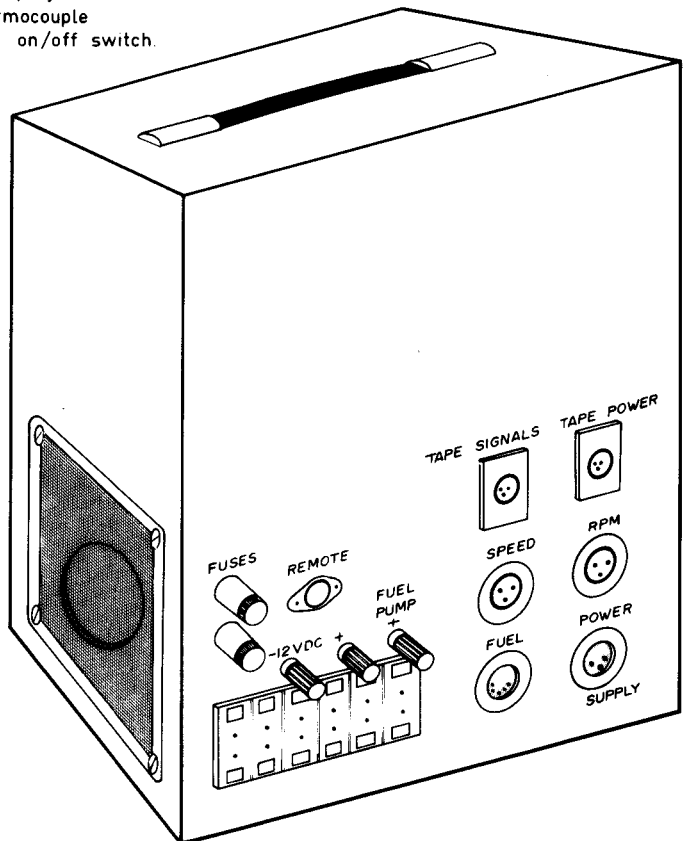


Figure 31: FERIC DATAMASTER. Rear view: Outlets for the pulse sending unit, power supply and Datalogger wires. The thermocouple outlets are located beneath the three VDC terminals.

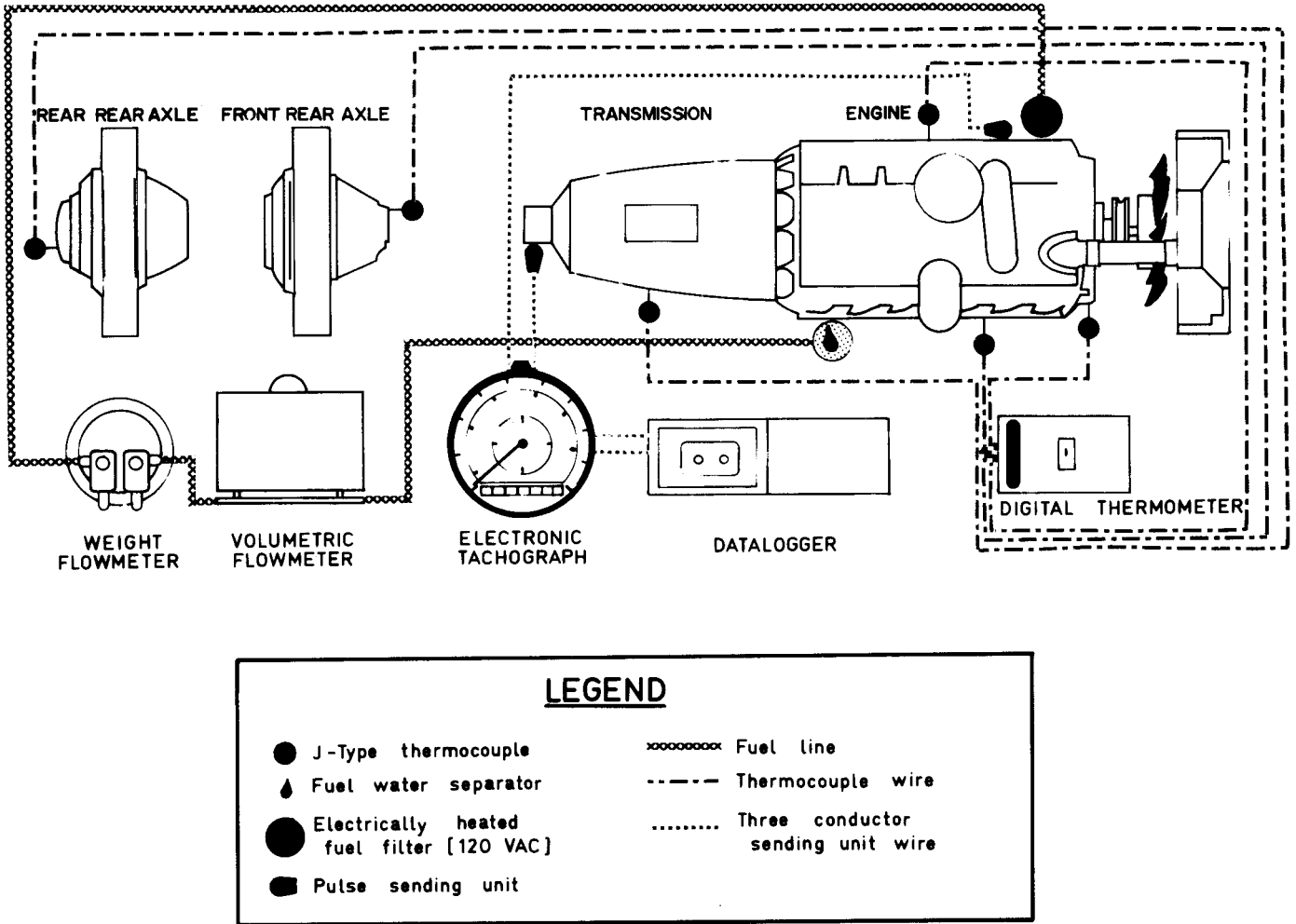


Figure 32: Connection scheme and diagram of measuring and logging instruments mounted on the vehicle.

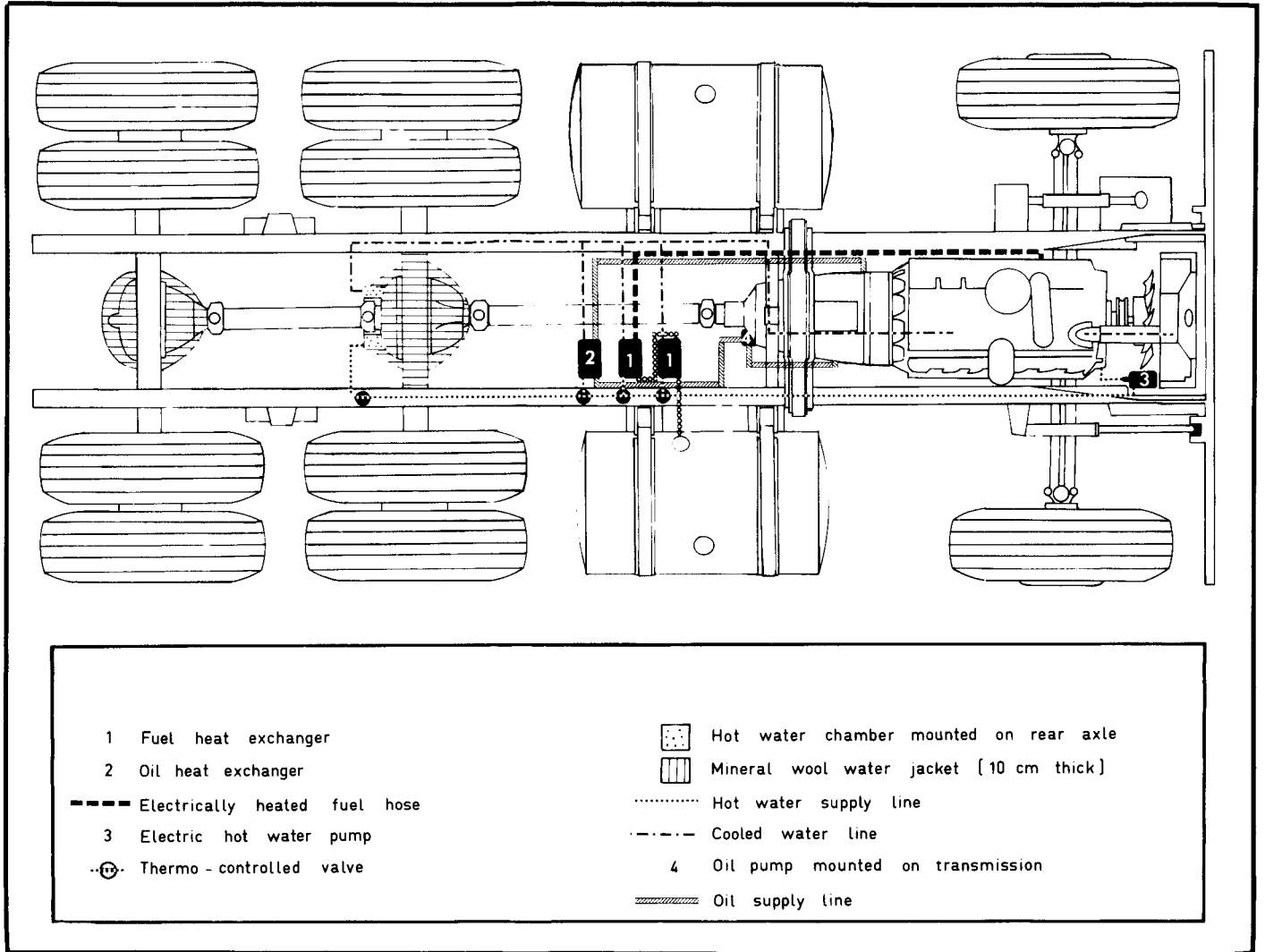


Figure 33: Diagram of equipment used to heat drive train components.

DEFINITIONS OF SYMBOLS

- a - Coefficient for the rate of increase of losses as determined by power transmission velocity, daN*s/m.
- a_a - Wheel acceleration, m/sec².
- b - Resisting moment lever, m.
- C_{CR} - Coefficient of resistance due to camber.
- C_{FRO} - Frontal resistance coefficient.
- C_{SD} - Coefficient owing to ground distorsion resistance.
- C_{SS} - Coefficient of resistance caused by side slip.
- C_{UC} - Undercarriage coefficient.
- D - Distance, m.
- d_{rs} - Road surface dispersal.
- F_a - Acceleration force daN.
- F_{AR} - Force of frontal resistance of moving vehicle, daN.
- F_{BEF} - Total brake force (brake and engine), daN.
- F_{DTR} - Force of drive train resistance, daN.
- F_{EBR} - Braking effort supplied by the engine, daN.
- F_{GR} - Grade resisting force, daN.
- F_I - Force of inertia, daN.
- F_{ir} - Force of inertia of rotating wheels, daN.

- F_{MBR} - Braking effort of the main braking system, daN.
- F_{MT} - Maximum value of tractive effort, daN.
- F_{OC} - Force corresponding to oil churning losses in power transmission system.
- F_{OC}° - Force of resistance corresponding to oil churning at near zero speeds, daN.
- F_{OUT} - Engine output force, daN.
- F_{RR} - Force of rolling resistance, daN.
- F_{rr} - Force of resistance in bearings of all non-drive wheels, daN.
- F_{SA} - Force of ground adhesion, daN.
- F_{ST} - Force at drive wheels under steady running conditions, daN.
- $F_{ST}(v_r)$ - Force at drive wheels at given road speed v_r , daN.
- F_T - Total wheel dynamic driving force, daN.
- F_{TR} - Total resisting force of driving tires on the ground (including air and rolling resistances at a given speed), daN.
- f_{AR} - Air resistance coefficient.
- Δf_C - Increment of coefficient f_{OS} by resistance through camber of front (drive) wheels.
- Δf_{GD} - Increment of coefficient f_{OS} through that part of resistance due to ground distortion.
- Δf_M - Increment of coefficient f_{OS} through application of torque to drive wheels.
- f_{OS} - Coefficient of rolling resistance at low speeds.
- f_{RR} - Rolling resistance coefficient.
- Δf_{SV} - Increment of coefficient f_{OS} through vibration in the suspension (tires and springs).
- Δf_{ur} - Increment of coefficient f_{OS} through unevenness of the road surface.
- Δf_{vr} - Increment of coefficient f_{OS} through increase in road speed.
- Δf_{δ} - Increment of coefficient f_{OS} by resistance through side slip angle of front (drive) wheels.

- G_L - Payload, daN.
- G_T - Total vehicle mass, daN.
- G_{TA} - Tare mass of the vehicle.
- G_W - Rated load per wheel, daN.
- g - Gravitational acceleration, m/sec^2 .
-
- i_{RA} - Rear axle ratio.
- i_{TR} - Transmission ratio.
-
- J_a - Vehicle acceleration m/s^2 .
- J_{DT} - Moment of inertia of the drive train, $daN \cdot m \cdot sec^2$.
- J_E - Engine moment of inertia, $daN \cdot m \cdot sec^2$.
- J_{WT} - Moment of inertia of tire with wheel, $daN \cdot m \cdot sec^2$.
- J_{WTDT} - Moment of inertia of wheels with drive train, $daN \cdot m \cdot sec^2$.
- $J_{\Sigma WT}$ - Moment of inertia of all tires with wheels, $daN \cdot m \cdot sec^2$.
-
- K - Coefficient for rate of increment of air resistance losses as a function of squared speed, $daN \cdot s^2/m^4$.
- k - Coefficient for rate of increment of rolling resistance as a function of squared speed, $daN \cdot s^2/m^2$ ($daN \cdot s^2/m^2$).
-
- M_A - Moment applied to drive wheels (before loss at the ground), $daN \cdot m$.
- M_{ES} - Rotating moment of engine under steady running conditions, $daN \cdot m$.
- M_{EV} - Engine rotating moment under variable running conditions, $daN \cdot m$.

- M'_{EV} - Engine moment at point ', daN·m.
- M''_{EV} - Engine moment at point '', daN·m.
- M_R - Moment of resistance at a given moment, daN·m.
- $(M_R^r)'$ - Total vehicle moment of resistance at point '.
- $(M_R^r)''$ - Total vehicle moment of resistance at point ''.
- M_{RW} - Rotating moment of wheels, daN·m.
- M_{TW} - Moment at traction wheels.
- M_{WD} - Moment at drive wheels (on the ground), daN·m.
-
- m_L - Mass of useful load, daN, (G_L/g).
- m_T - Total mass of loaded vehicle, daN, (G_T/g).
- m_{TA} - Tare mass of vehicle combination, daN, (G_{TA}/g).
- m_Z - Number of cylindrical gears in mesh.
-
- N_{EF} - Effective power of engine without accessories, kW.
- N_{ESP} - Specific power, kW/ton.
- N_{OUT} - Engine output power (engine mounted in truck), kW.
- N_{TL} - Power loss in power transmission system, kW.
- N_W - Power at wheels, kW.
- n_E - Engine rotating velocity, RPM.
- n_w - Number of wheel revolutions for distance D.
-
- o - Number of universal joints.
-
- P_w - Tire inflation pressure, daN/m².
- P_d - Dynamic pressure on frontal area, daN/m².
- P_o - Standard barometric pressure (10 132.48 daN/m²).

- P_{tp}° - Oil churning resisting force at zero speed, daN.
- $P_{f\Sigma}^{\circ}$ - Rolling resistance force at near zero speed, daN.
- P_{fa}° - Force of tire rolling and drive train rotation resistance at near zero speed, $\text{daN}\cdot\text{s}^2/\text{m}^2$.
- P_{tp}° - Oil churning resisting force at a given speed, daN.
- Q - Fuel consumption on the road, kg/h.
- Q_E - Power consumption, kW.
- Q_{GR} - Resulting general force, daN.
- Q_{TA} - Fuel consumption related to transmission and axle oil churning losses, kg/h.
- R - Molar constant of gases.
- R_G - Reaction at the ground, daN.
- R_{GT} - Reaction at ground (with applied torque), daN.
- R_{GW} - Reaction at ground due to weight on wheel, daN.
- R_{OCC} - Oil churning resistance calculated from fuel consumption, daN.
- R_W - Reaction at ground to the weight on the wheel, m.
- r - Road curve radius, m.
- r_{FR} - Free tire radius, m (meters).
- r_{LD}^M - Loaded tire radius (dynamic) with applied torque, m.
- r_{LK}° - Loaded tire radius (kinematic) without applied torque, m.
- r_{LS} - Loaded tire radius (static), m.
- r_{FR} - Free inflated tire radius, m.
- S - Maximum frontal area, m^2 .
- T - Absolute temperature in $^{\circ}\text{K}$.
- T_o - Standard air temperature (288°K).
- t - Time, sec.
- t_D - Time taken to travel distance D.
- t_o - Oil temperature, $^{\circ}\text{C}$.

- v_{AIR} - Air velocity, m/sec.
- v_r - Road speed, m/sec.
- v_r' - Road speed at point ', m/sec.
- v_r'' - Road speed at point '', m/sec.

- x - Number of bevel gears in mesh.

- Z_w - Number of wheels.

- α - Degree of incline of road, degrees.

- β - Camber, in degrees.

- γ - Density of air.

- δ - Angle of side slip.
- δ_{RM}' - Coefficient for calculating vehicle rotating masses.
- δ_{RM} - Coefficient for calculating rotating masses (free wheeling truck).

- ϵ - Inclination of slope during tests to determine moment J_r .

- μ - Angle of depression of pedal.

- η_a - Efficiency coefficient of engine acceleration.
- η_{A1} - Efficiency coefficient of forward-rear axle.
- η_{A2} - Efficiency coefficient of rear-rear axle.
- η_{BG}^n - Efficiency of bevel gears in mesh.
- η_{CG}^m - Efficiency of cylindrical gears in mesh.
- η_{DT} - Efficiency coefficient of drive train (total).
- η_{EA} - Overall efficiency coefficient of engine with accessories (excluding heat and engine mechanical losses).

- η_{EAT} - Efficiency coefficient through increase in engine ambient temperature.
- η_{EC} - Efficiency coefficient of engine accessories.
- η_{FR} - Efficiency coefficient for friction in power transmission system (with applied torque).
- η_{MT} - Maximum efficiency of one tire.
- η_{OCL} - Oil churning efficiency coefficient.
- η_{PL} - Efficiency coefficient of power transmission.
- η_{SL} - Efficiency coefficient attributable to height above sea level.
- η_{TL} - Efficiency coefficient of transmission losses.
- η_{TW} - Efficiency coefficient of traction wheel.
- η_{UJ} - Efficiency coefficient of universal joint.

- ϕ - Coefficient of tire adhesion to ground.

- λ - Tangential elasticity modulus of tires.

- ρ - Volumetric mass of air for non-standard conditions, $\text{daN}\cdot\text{s}^2/\text{m}^4$.
- ρ_0 - Volumetric mass of air in $\text{daN}\cdot\text{s}^2/\text{m}^4$ for standard conditions ($0.125 \text{ daN}\cdot\text{s}^2/\text{m}^4$).

- ψ - Overall coefficient of resistance (slope and rolling).

- ω_{EN} - Engine angular velocity, sec^{-1} .

REFERENCES

1. Caubet, J.J. 1964. La théorie et pratique industrielle du frottement. Paris: Dunod-Technip. 356 pp.
2. Conference on Driveline Engineering. In Institution of Mechanical Engineers. Proceedings, vol. 184, part 31, 1969-1970. London. 556 pp.
3. Ljubic, D.A. Analysis of Productivity and Cost of Forestry Transportation. PART ONE: Pilot Study to Determine the Factors for Analysis of Commercial Vehicle Power Consumption and Road Performance. For. Eng. Res. Inst. of Can. Tech. Rep. No. TR-53, June 1982. 49 pp.
4. Reimpell, Jörusen. 1982. Jahrwerktechnik. Wüzburg: Vogel-Verlag. 892 pp.
5. Smith, Gary L. 1970. Commercial Vehicle Performance and Fuel Economy. Warrendale, Pa.: Society of Automotive Engineers. Technical Paper 700194. 46 pp.
6. Tokarev, A.A. 1982. Toplivnaia ekonomitchnost i tiagovo-skorostnie katchestva avtomobilia. Moscow: Mashinostroenie. 218 pp.
7. Zakin, H. 1967. Prikladnaia teoria dvijenja avtopoezda. Moscow: Transport. 254 pp.